

Supporting information

" Novel sulfonamide derivatives as multitarget antidiabetic agents: Design, synthesis, and biological evaluation "

Mohammed Salah Ayoup*^{1,2}, Nourhan Khaled¹, Hamida Abdel-Hamid¹, Doaa A Ghareeb³, Samah A. Nasr³, Ahmed Omer^{4,5}, Amr Sonousi^{6,7}, Asmaa E. Kassab*⁶, Abdelazeem S. Eltaweil^{1,8}

¹ Department of Chemistry, Faculty of Science, Alexandria University, Alexandria, Egypt.

² Department of Chemistry, College of Science, King Faisal University, Al-Ahsa 31982, Saudi Arabia.

³ Bio-screening and preclinical trial lab, Biochemistry Department, Faculty of Science, Alexandria University, Alexandria, Egypt.

⁴ Polymer Institute of the Slovak Academy of Sciences, Dúbravská Cesta 9, 845 41 Bratislava, Slovakia.

⁵ Polymer Materials Research Department, Advanced Technology and New Materials Research Institute (ATNMRI), City of Scientific Research and Technological Applications (SRTA-City), New Borg El-Arab City, Alexandria 21934, Egypt

⁶ Department of Pharmaceutical Organic Chemistry, Faculty of Pharmacy, Cairo University, Kasr El-Aini Street, Cairo, P.O. Box 11562, Egypt.

⁷ University of Hertfordshire hosted by Global Academic Foundation, New Administrative Capital, Cairo, Egypt.

⁸ Department of Engineering, Faculty of Technology and Engineering, University of Technology and Applied Sciences, Sultanate of Oman.

*Corresponding authors: Email addresses: mayoup@kfu.edu.sa & mohammedsalahayoup@gmail.com,
asmaa.kassab@pharma.cu.edu.eg

Contents

1. ^1H , ^{13}C NMR and IR spectra of the synthesized compounds (Figures 1-48)	S3-S48
2. Equipment and analytical technique	S51
3. Biological procedures	S52
4. 2D diagram and 3D representation of molecular docking of all compounds in the binding pocket (PDB: 2QMJ).	S54
5. Biological activities detailed results	S60-S63
6. References	S63

1. ^1H , ^{13}C NMR and IR spectra of the synthesized compounds (Figures 1-48)

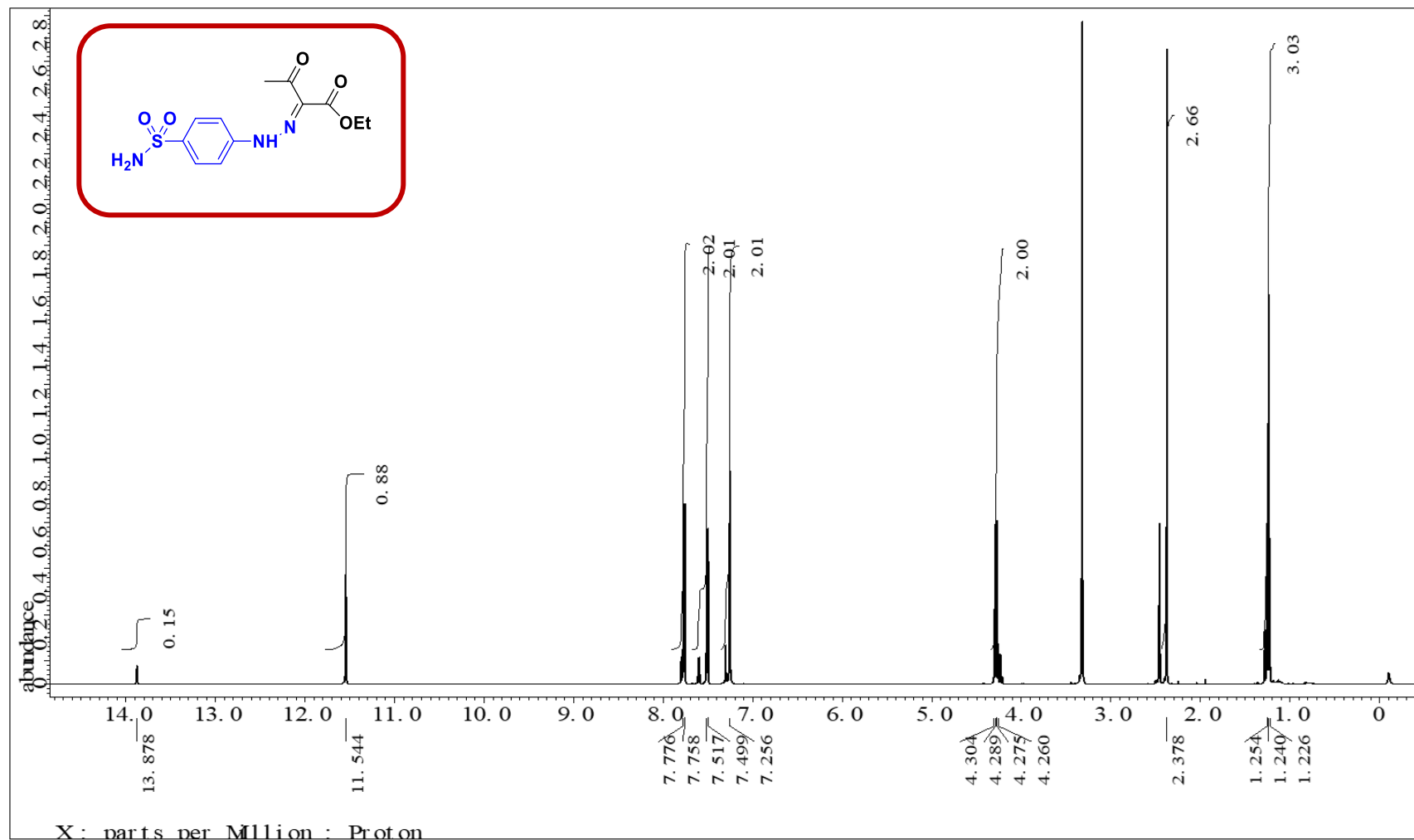


Fig. 1 ^1H -NMR spectrum (500 MHz, DMSO-d_6) of **2**.

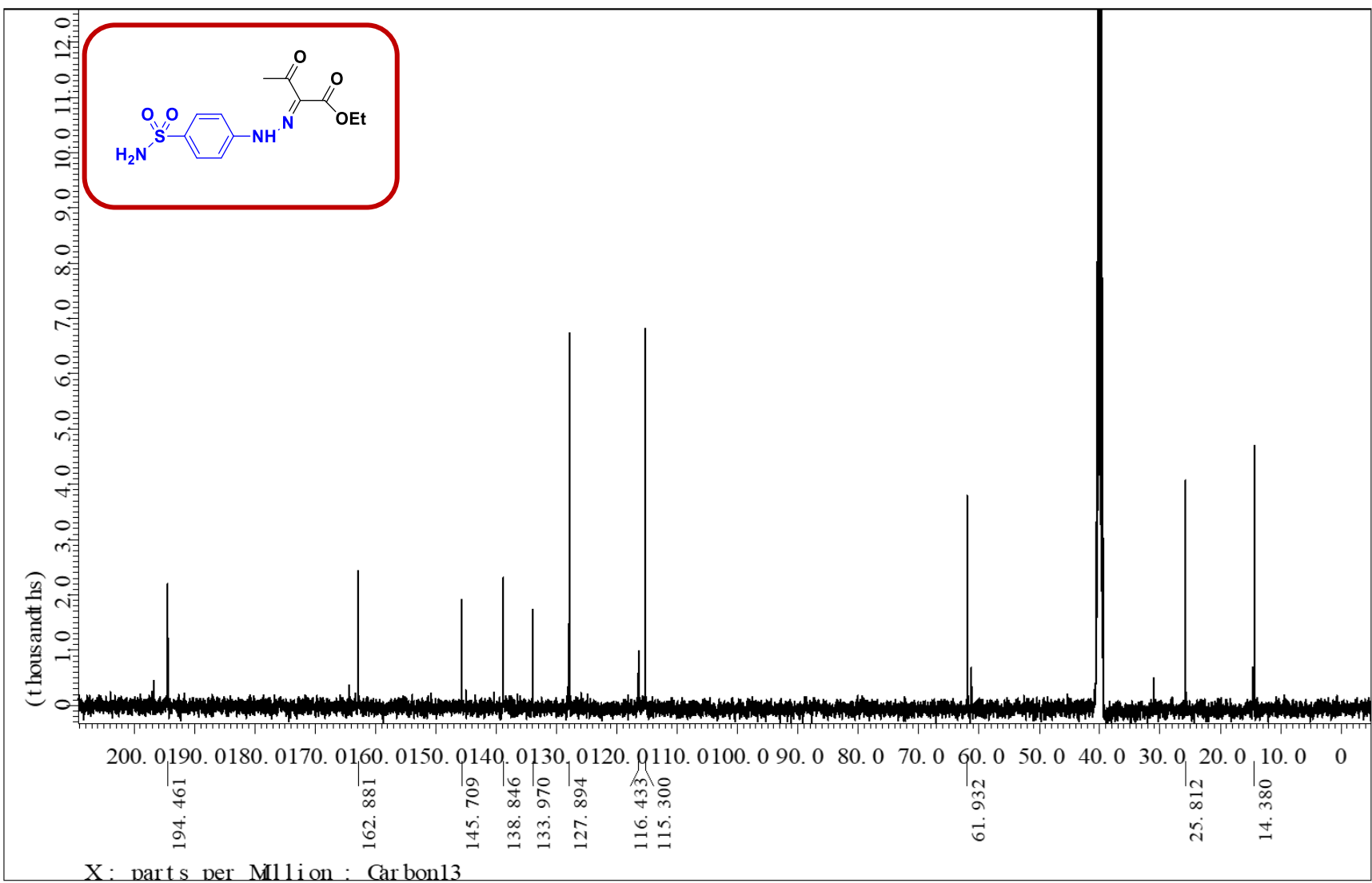


Fig. 2 ^{13}C -NMR spectrum (125 MHz, DMSO-d_6) of **2**.

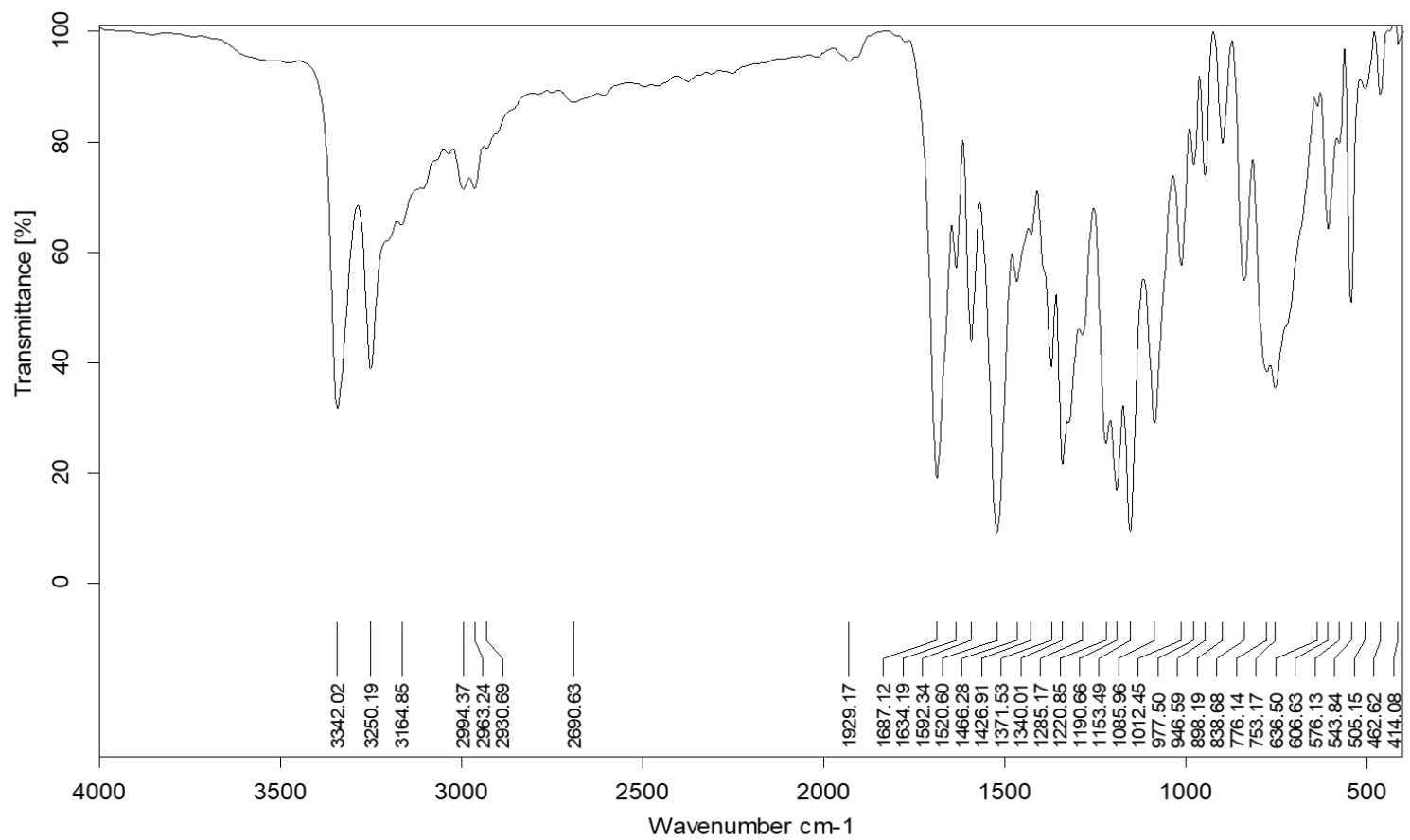


Fig. 3 IR spectrum of **2**.

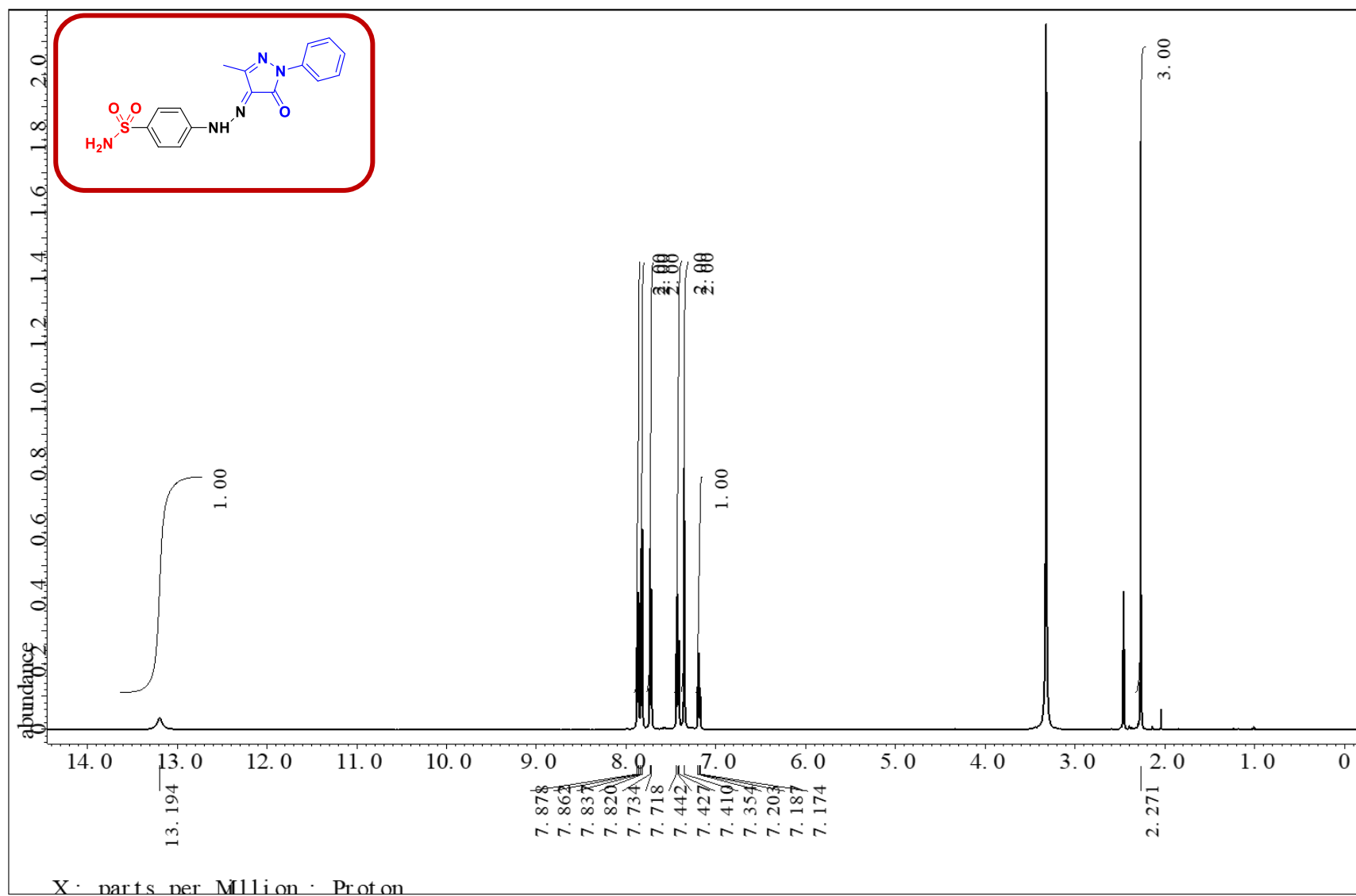


Fig. 4 $^1\text{H-NMR}$ spectrum (500 MHz, DMSO-d_6) of 3a.

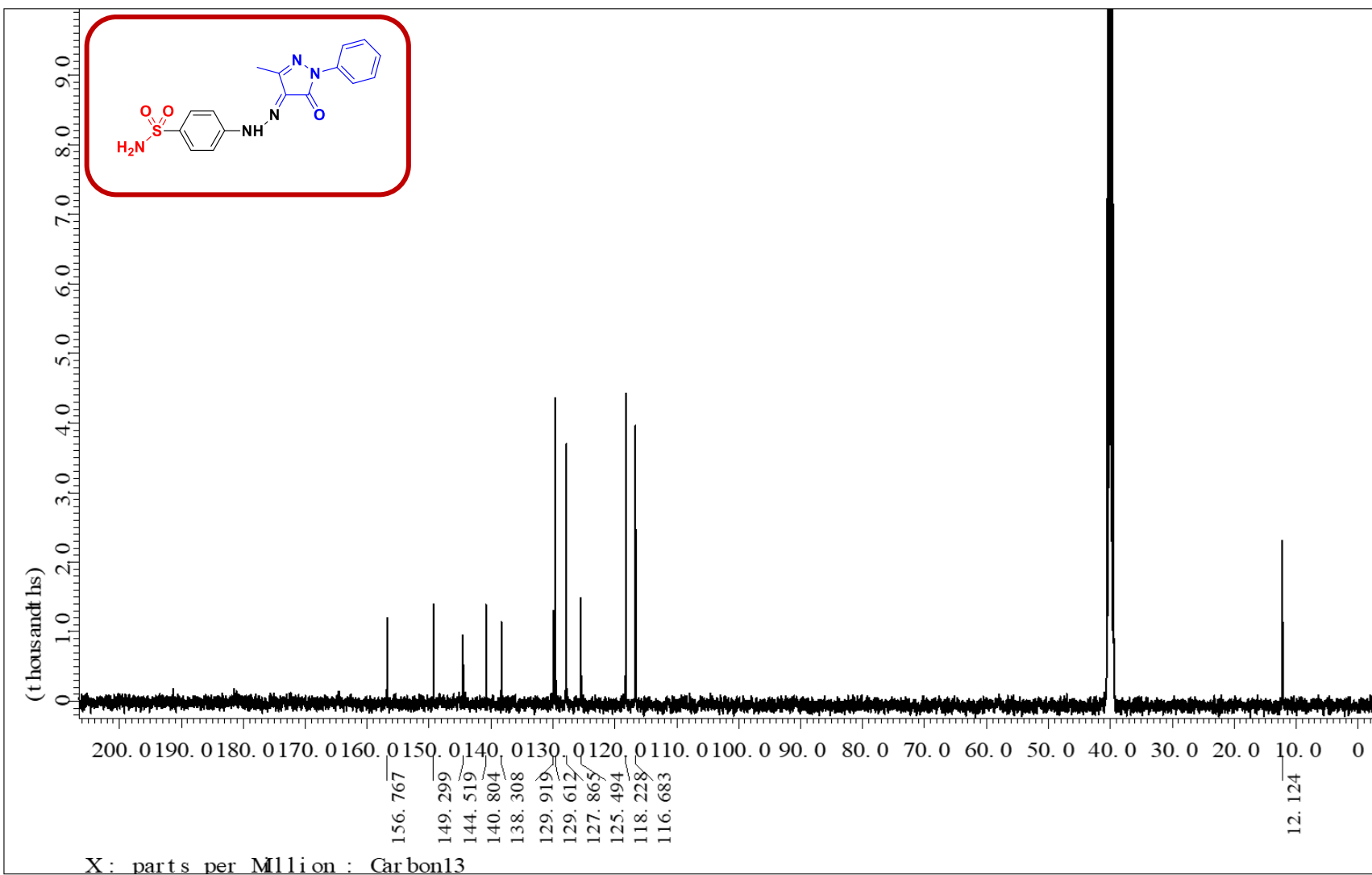


Fig. 5 ^{13}C -NMR spectrum (125 MHz, DMSO- d_6) of 3a.

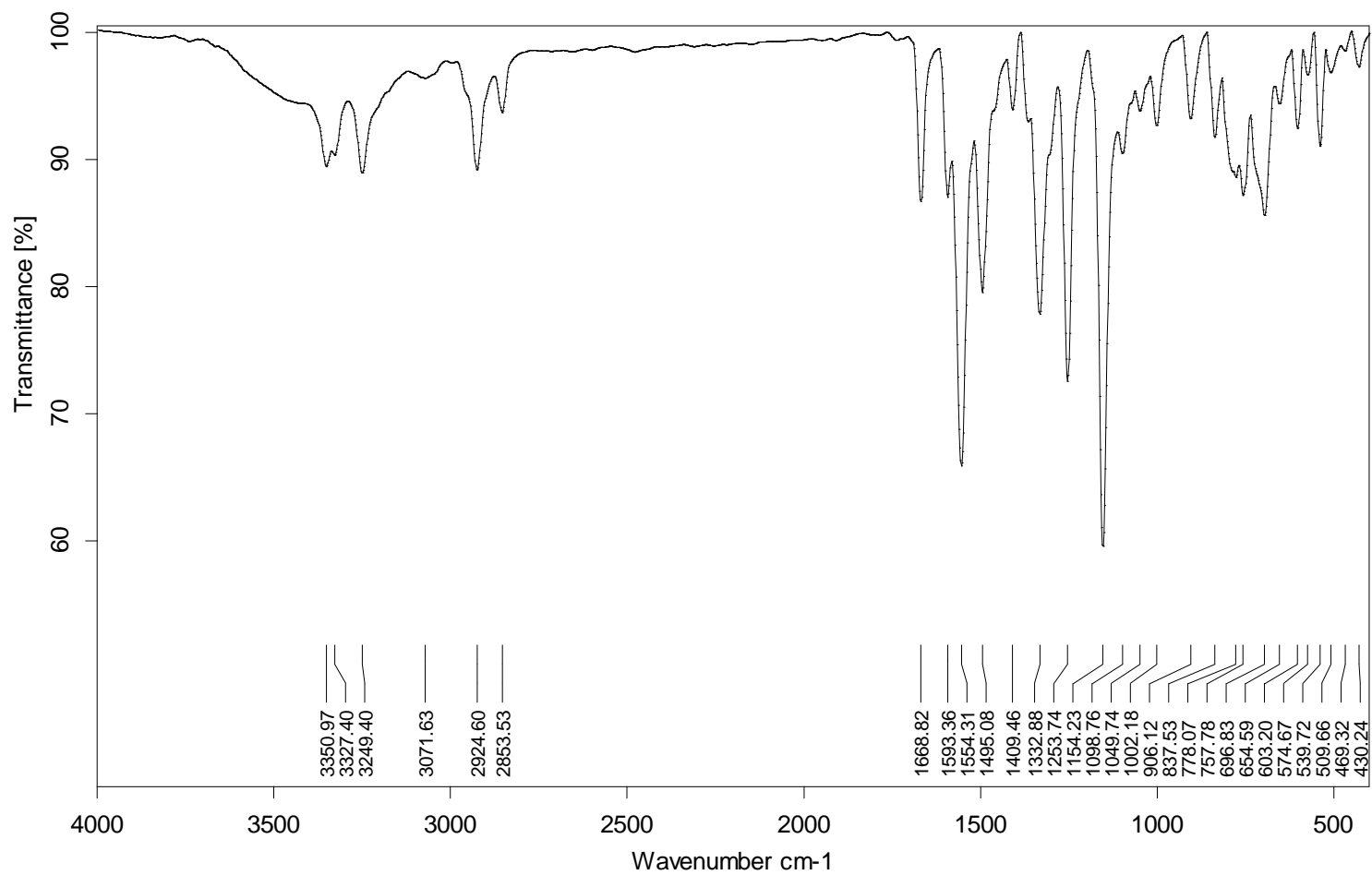


Fig. 6 IR spectrum of **3a**.

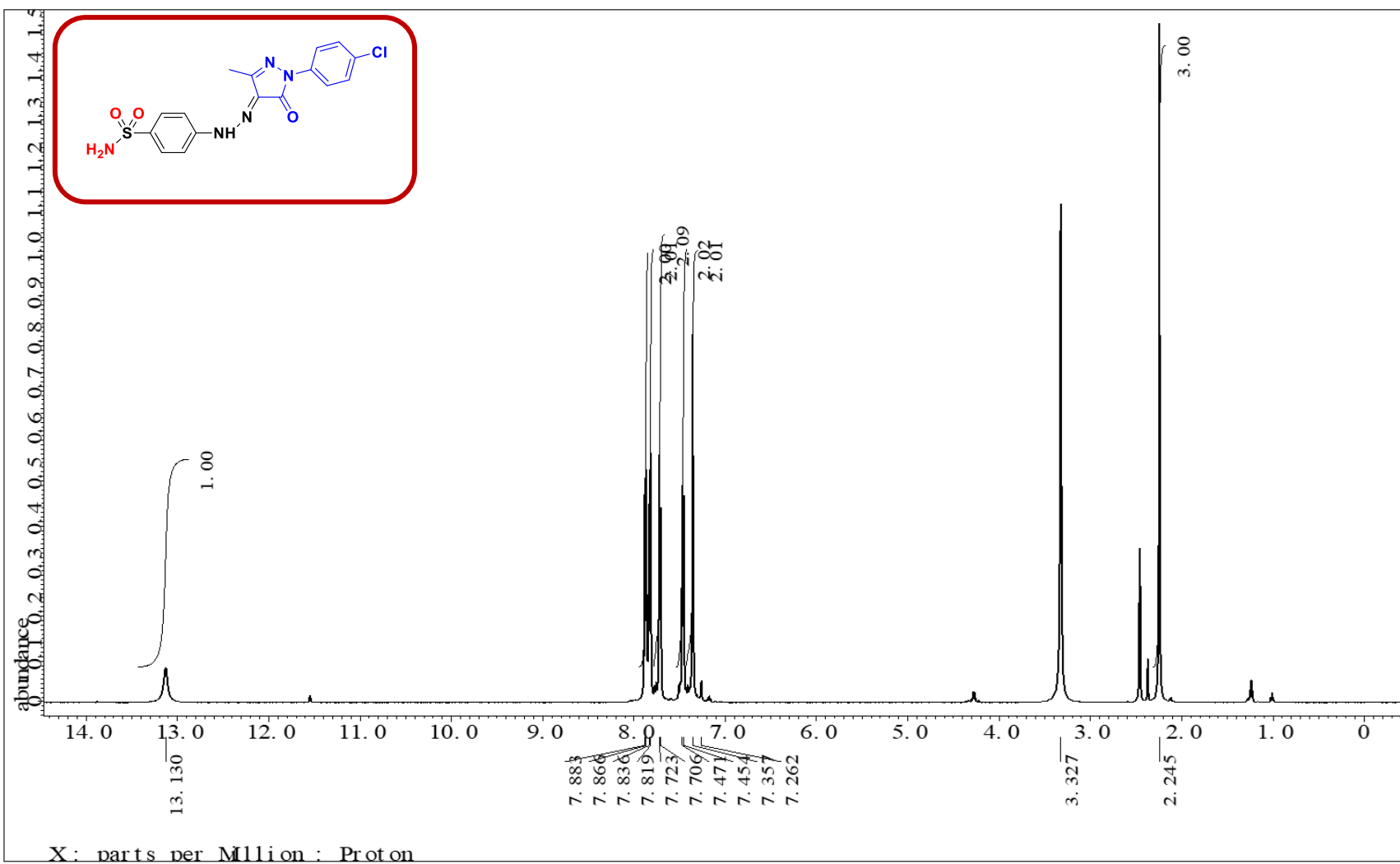


Fig. 7 $^1\text{H-NMR}$ spectrum (500 MHz, DMSO-d_6) of 3b.

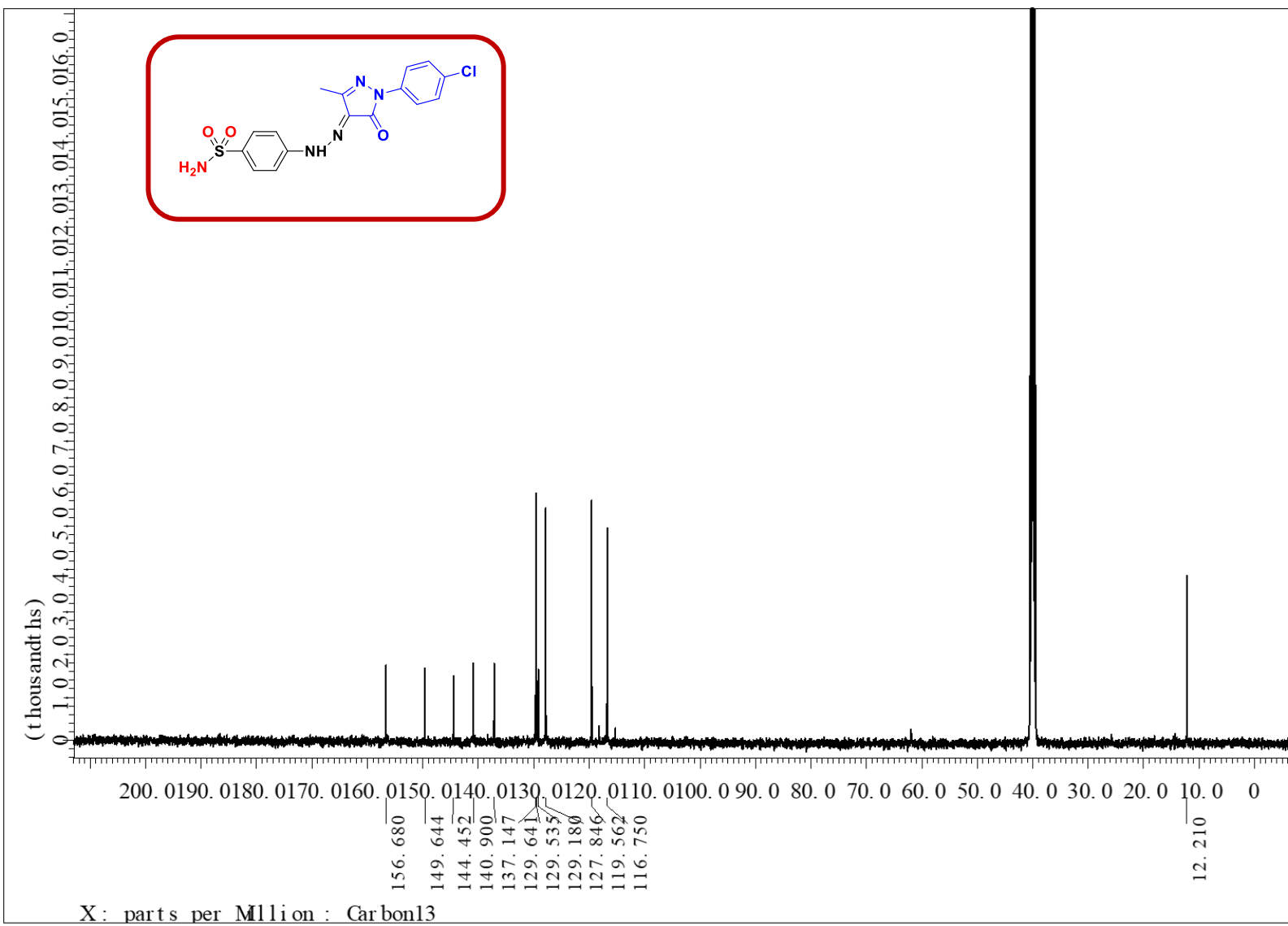


Fig. 8 ^{13}C -NMR spectrum (125 MHz, DMSO- d_6) of **3b**.

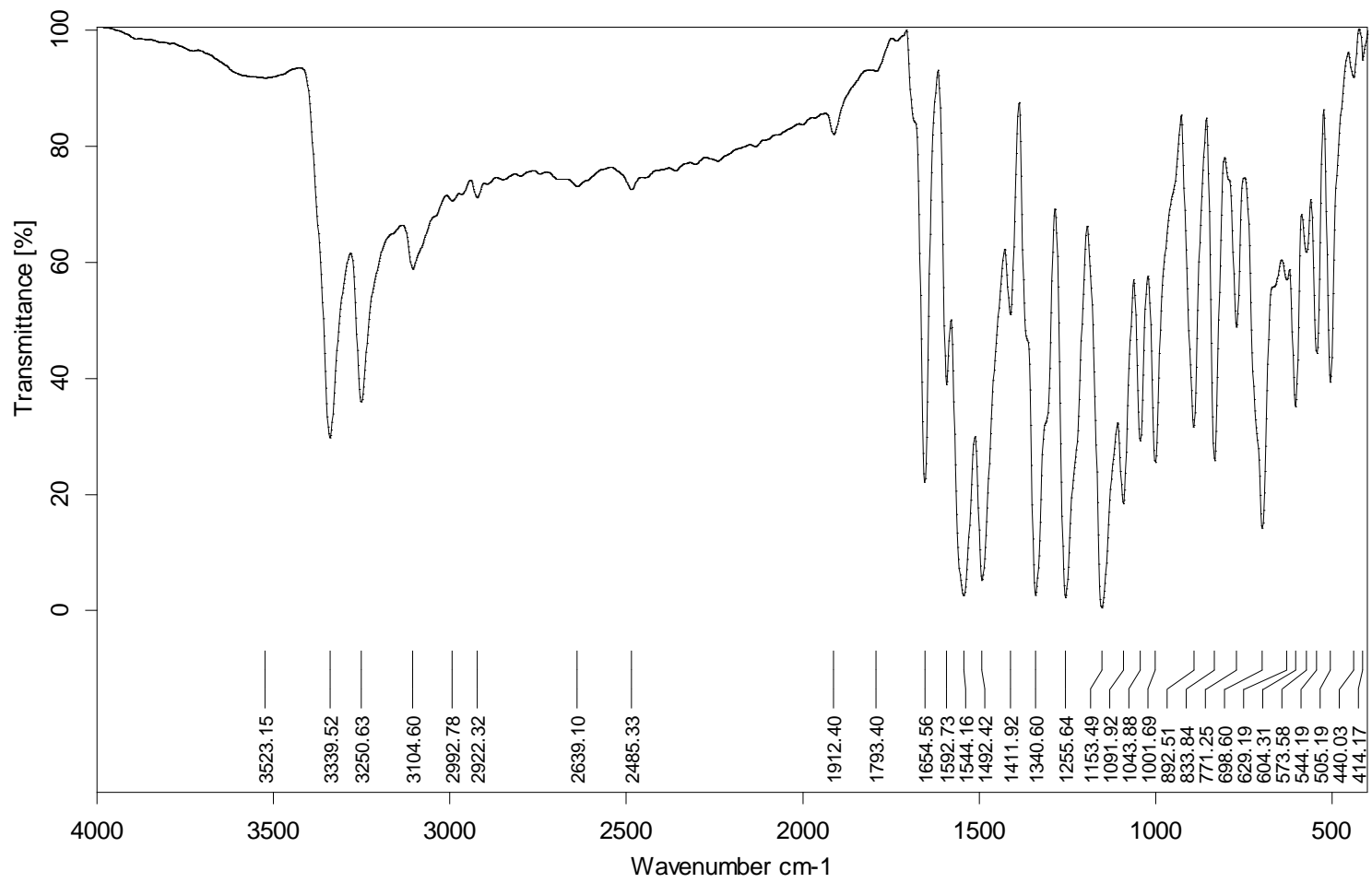


Fig. 9 IR spectrum of **3b**.

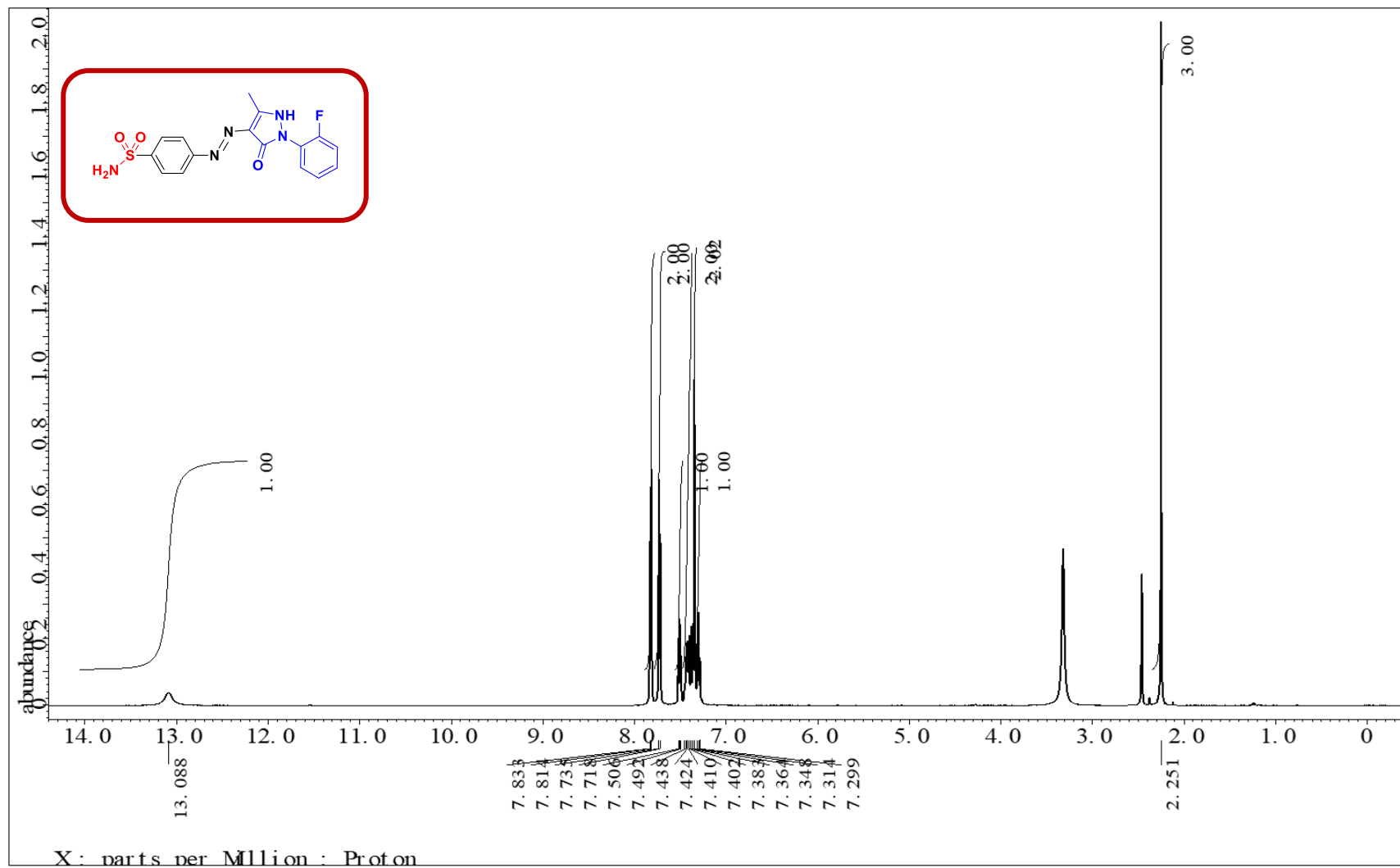


Fig. 10 ¹H-NMR spectrum (500 MHz, DMSO-d₆) of **3c**.

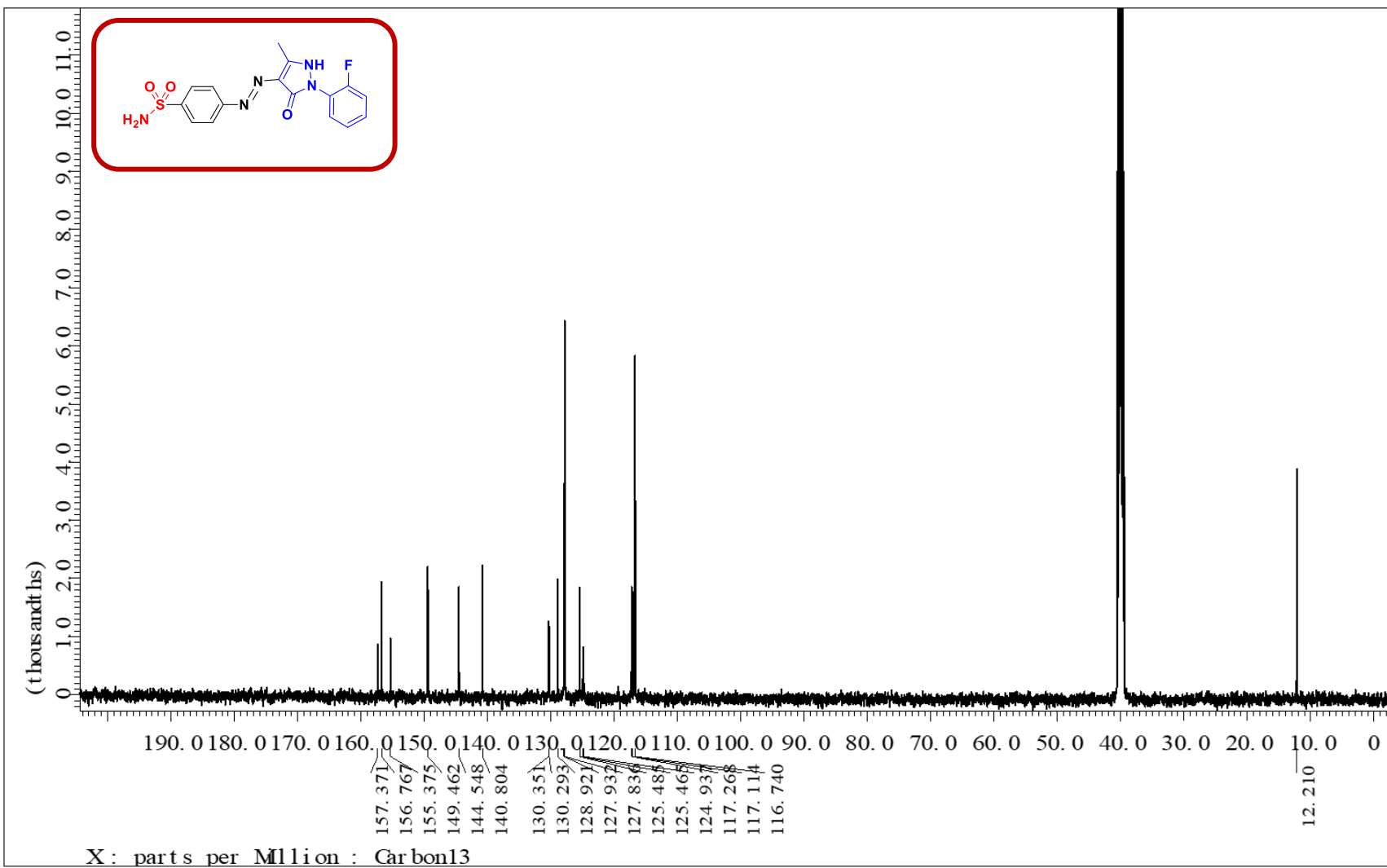


Fig. 11 ^{13}C -NMR spectrum (125 MHz, DMSO- d_6) of **3c**.

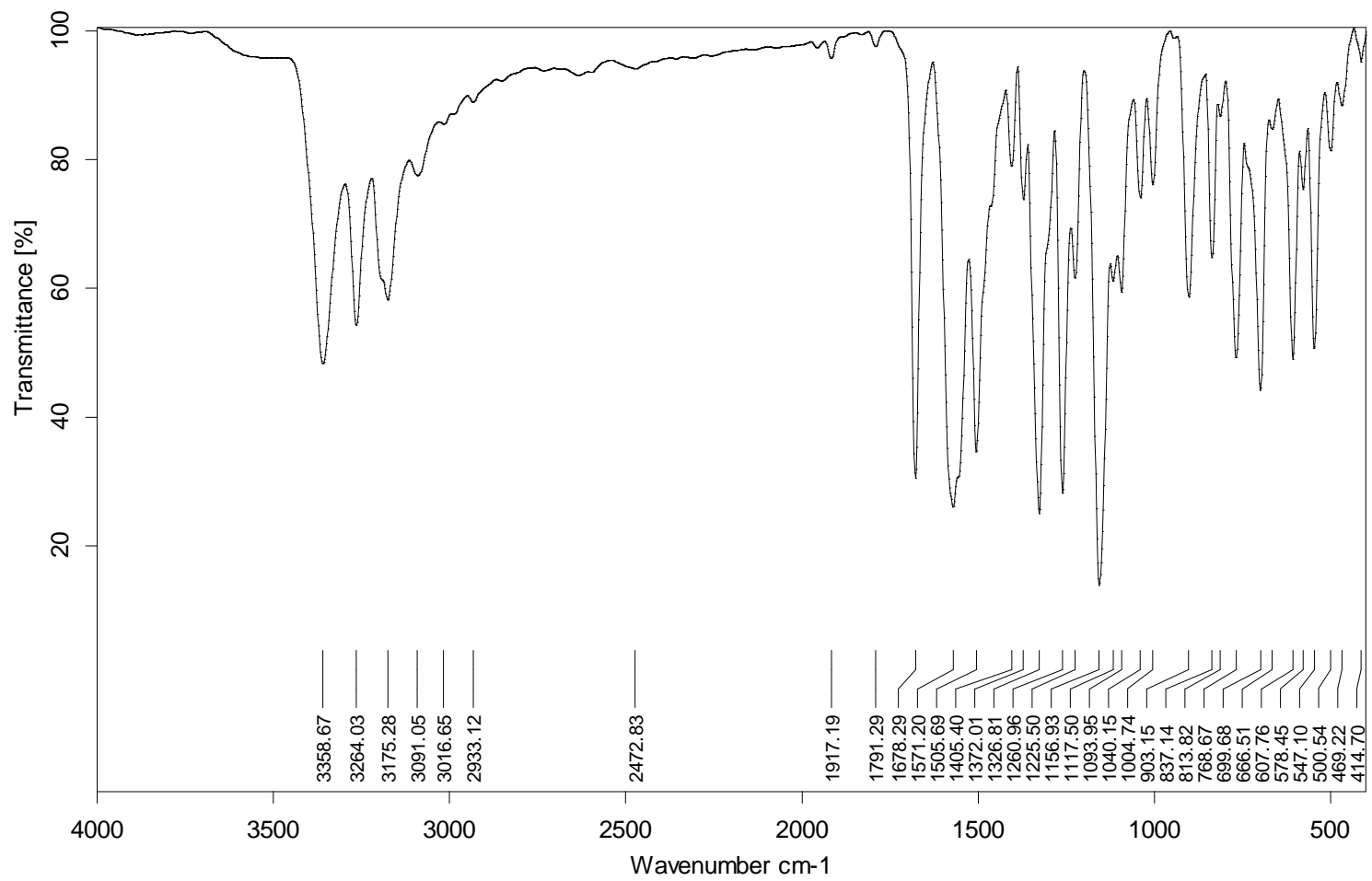


Fig. 12 IR spectrum of **3c**.

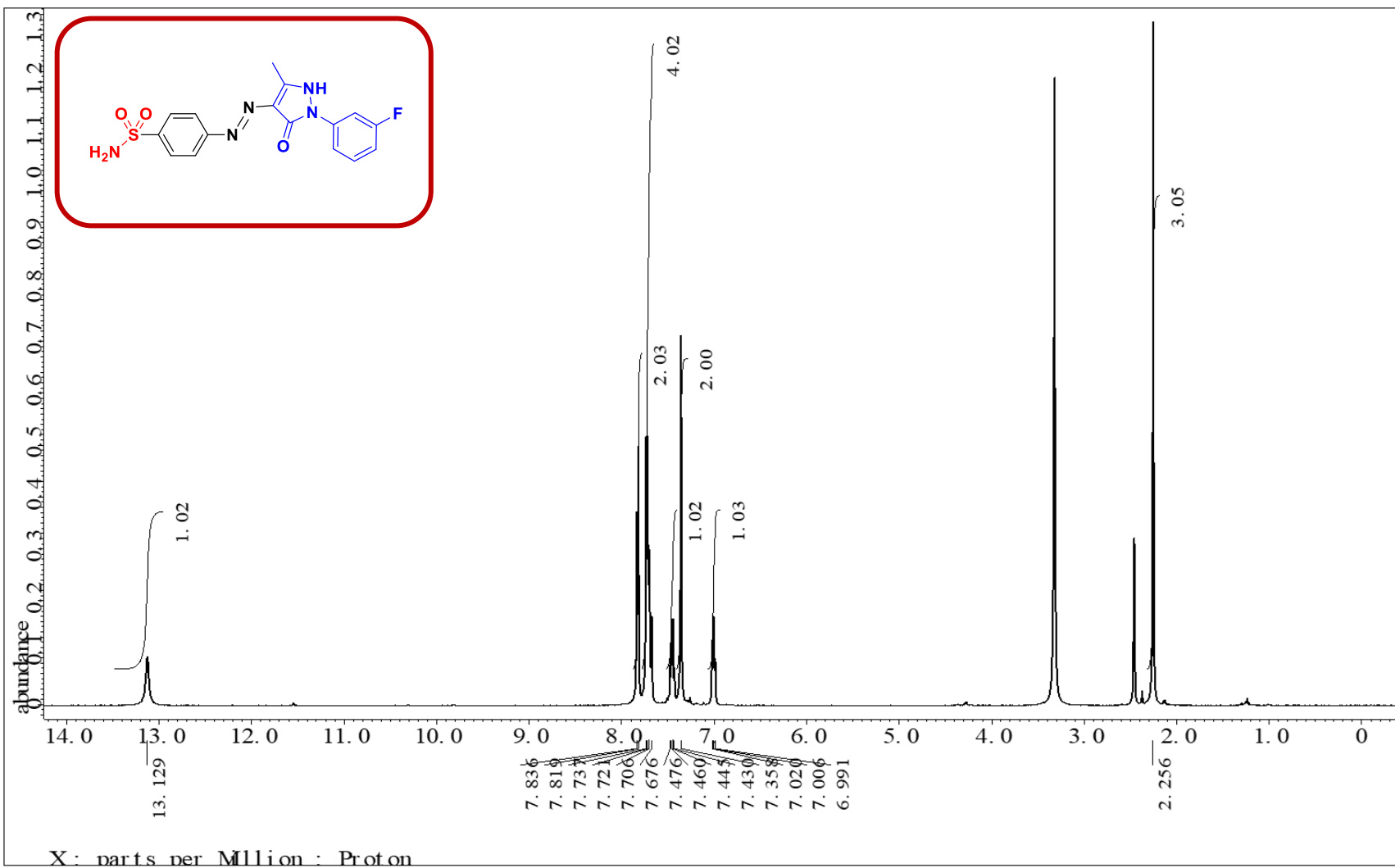


Fig. 13 ¹H-NMR spectrum (500 MHz, DMSO-d₆) of **3d**.

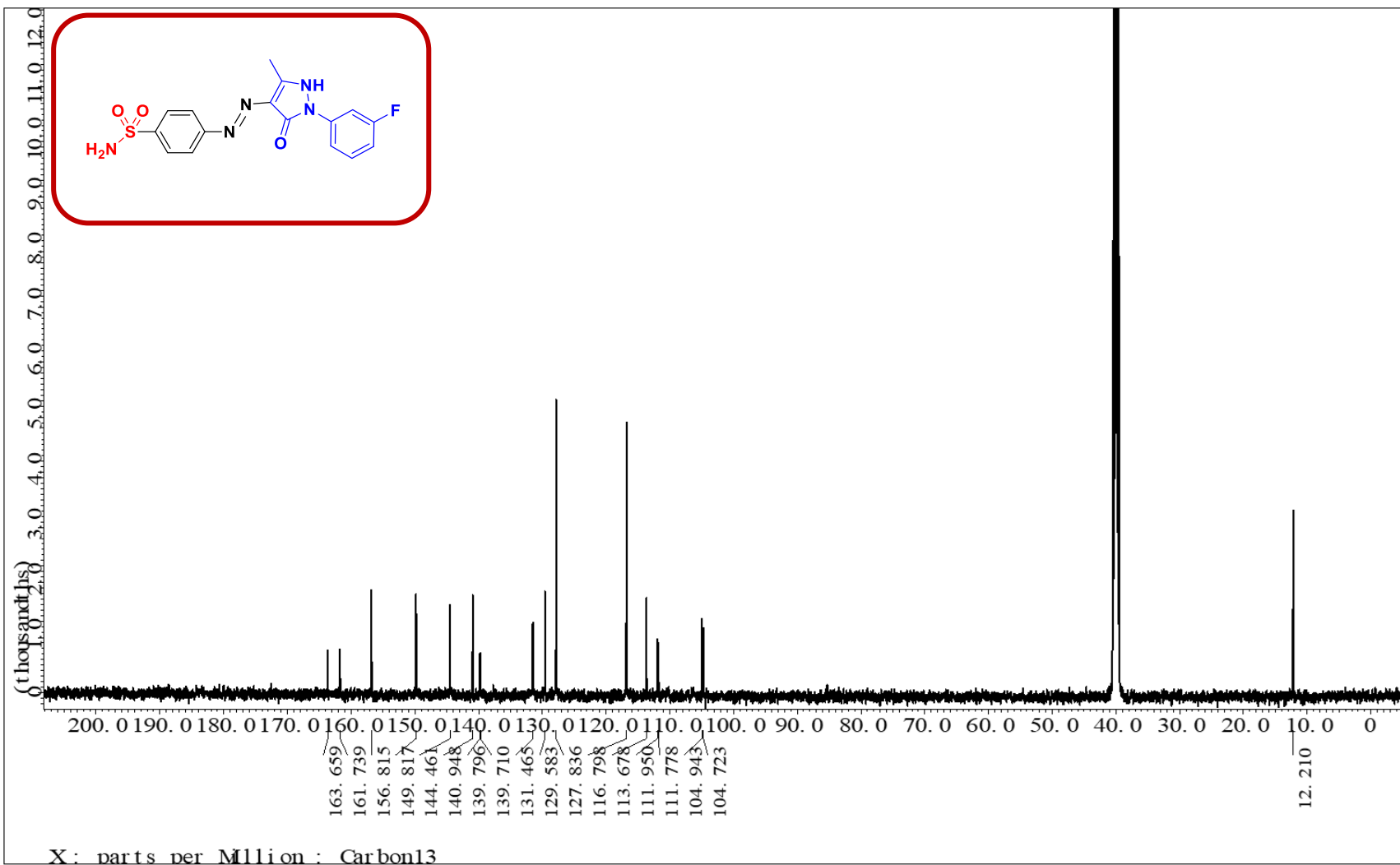


Fig. 14 ¹³C-NMR spectrum (125 MHz, DMSO-d₆) of 3d.

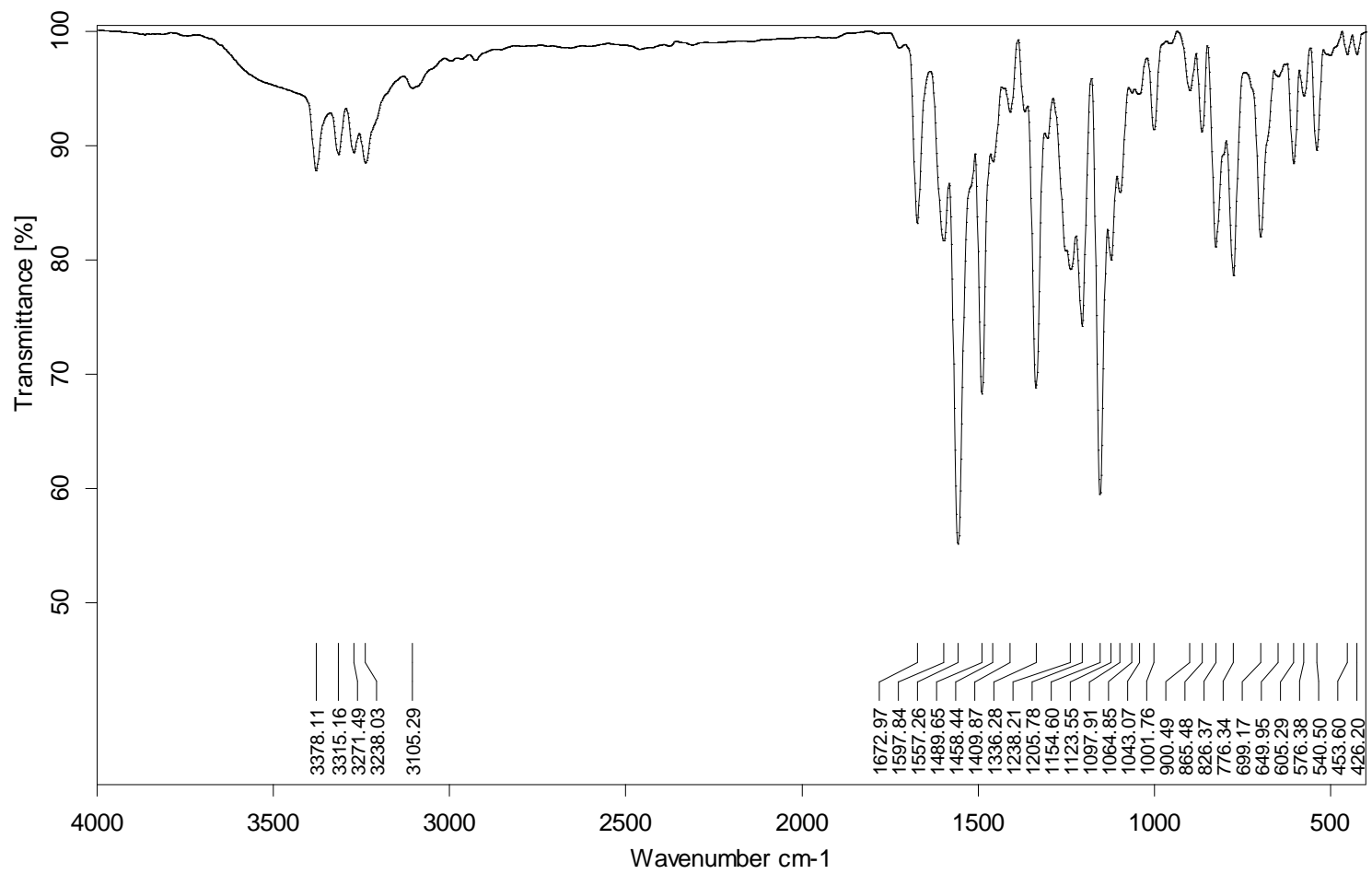


Fig. 15 IR spectrum of **3d**.

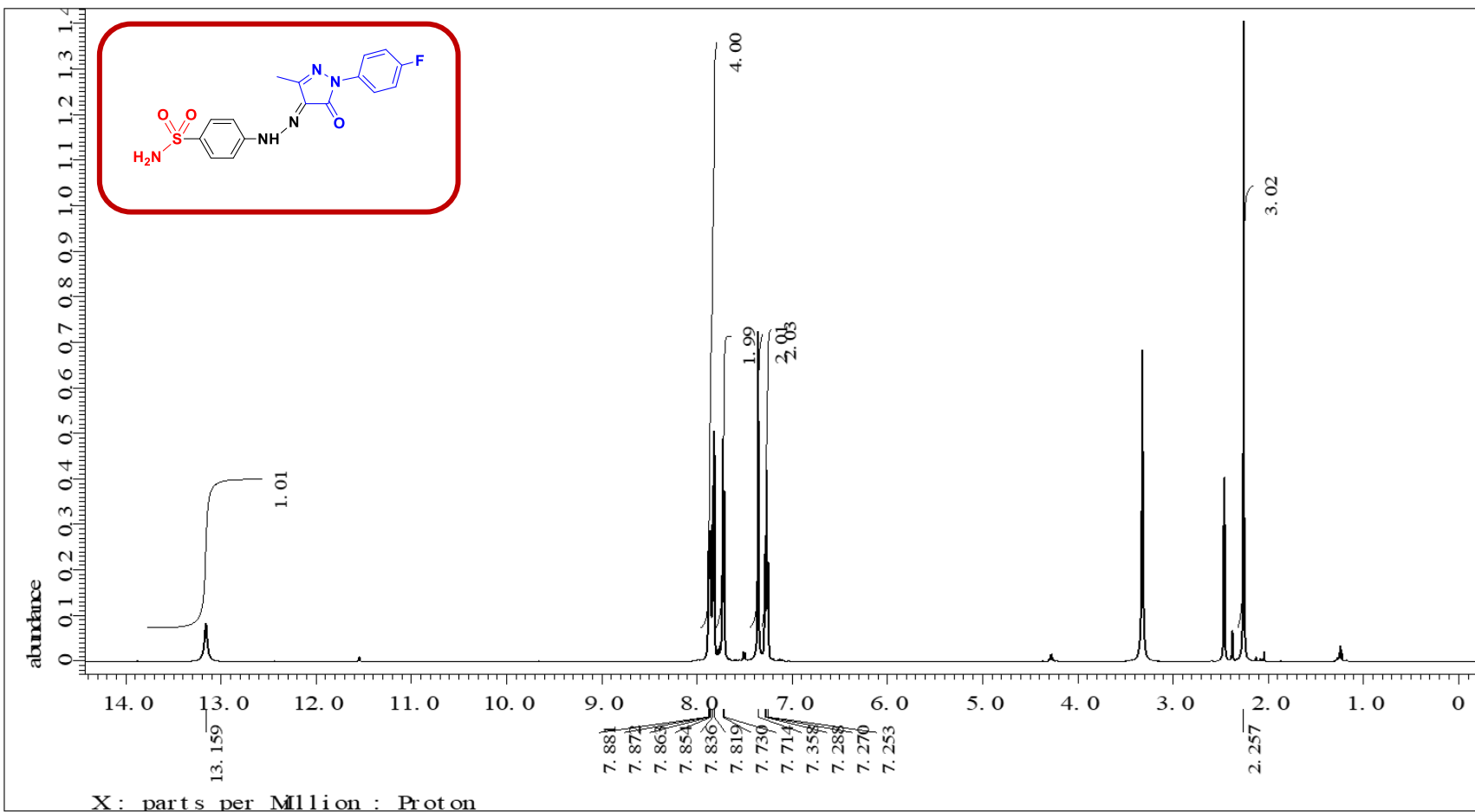


Fig. 16 ¹H-NMR spectrum (500 MHz, DMSO-d₆) of **3e**.

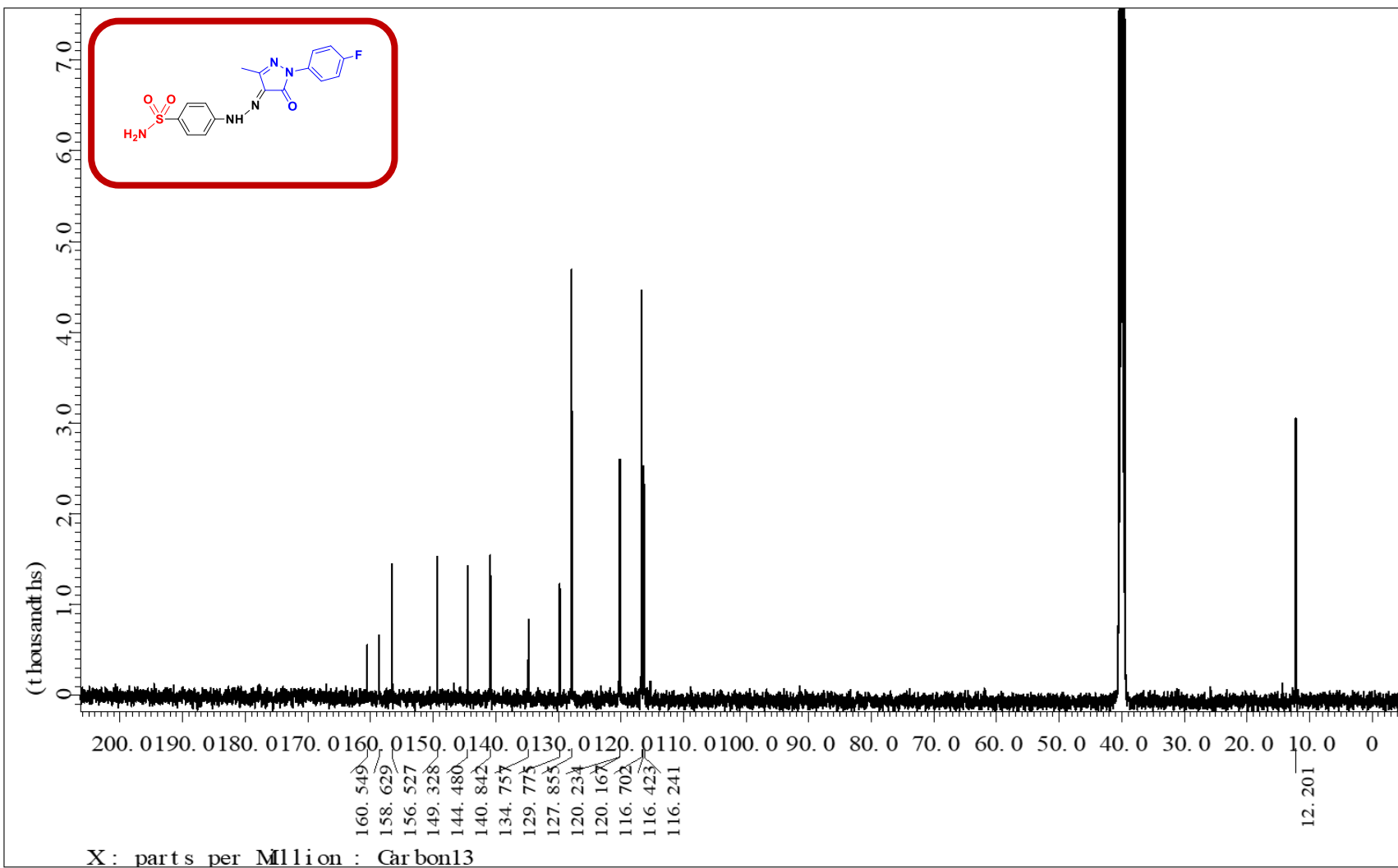


Fig. 17 $^{13}\text{C-NMR}$ spectrum (125 MHz, DMSO- d_6) of 3e.

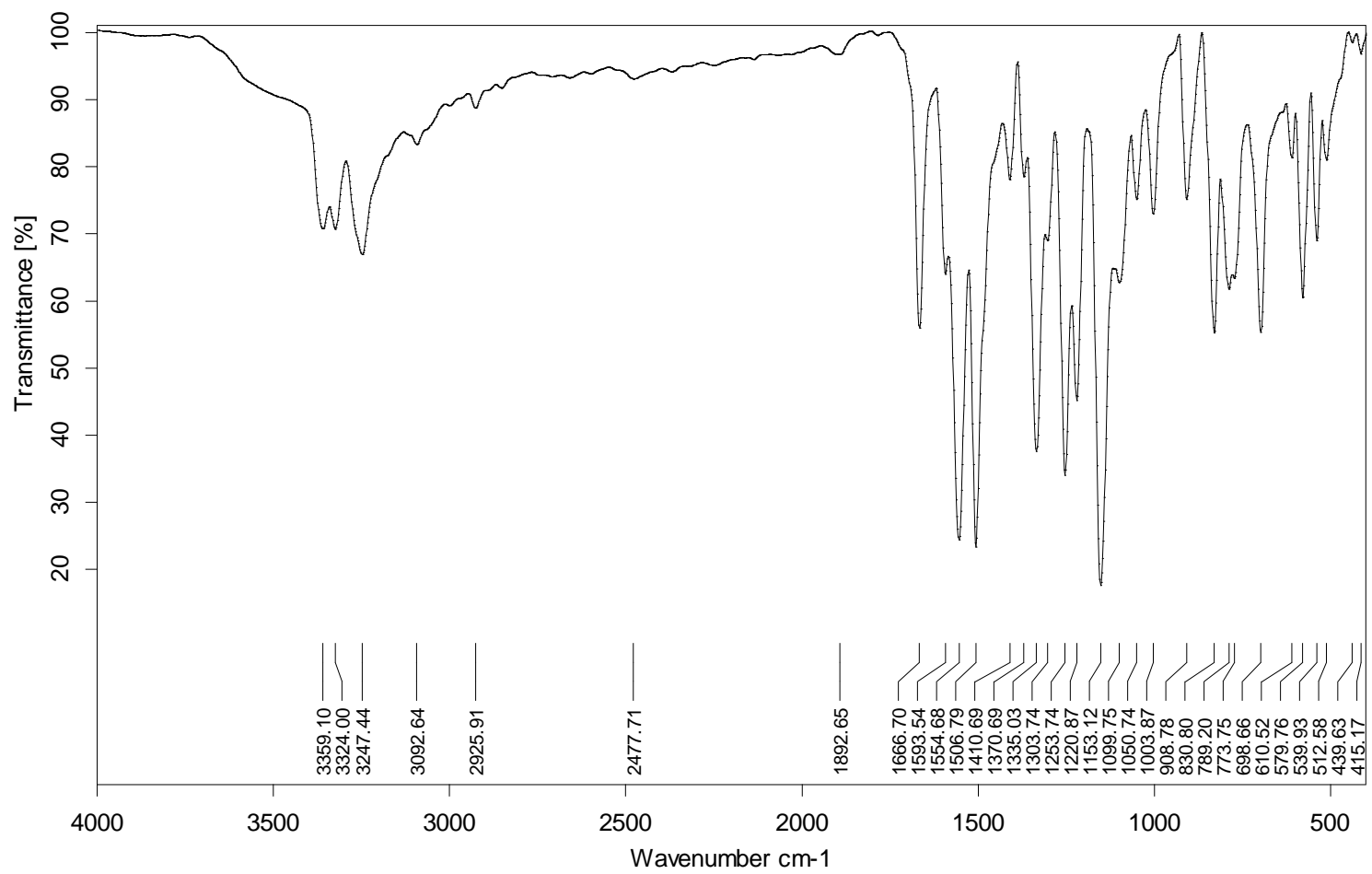


Fig. 18 IR spectrum of **3e**.

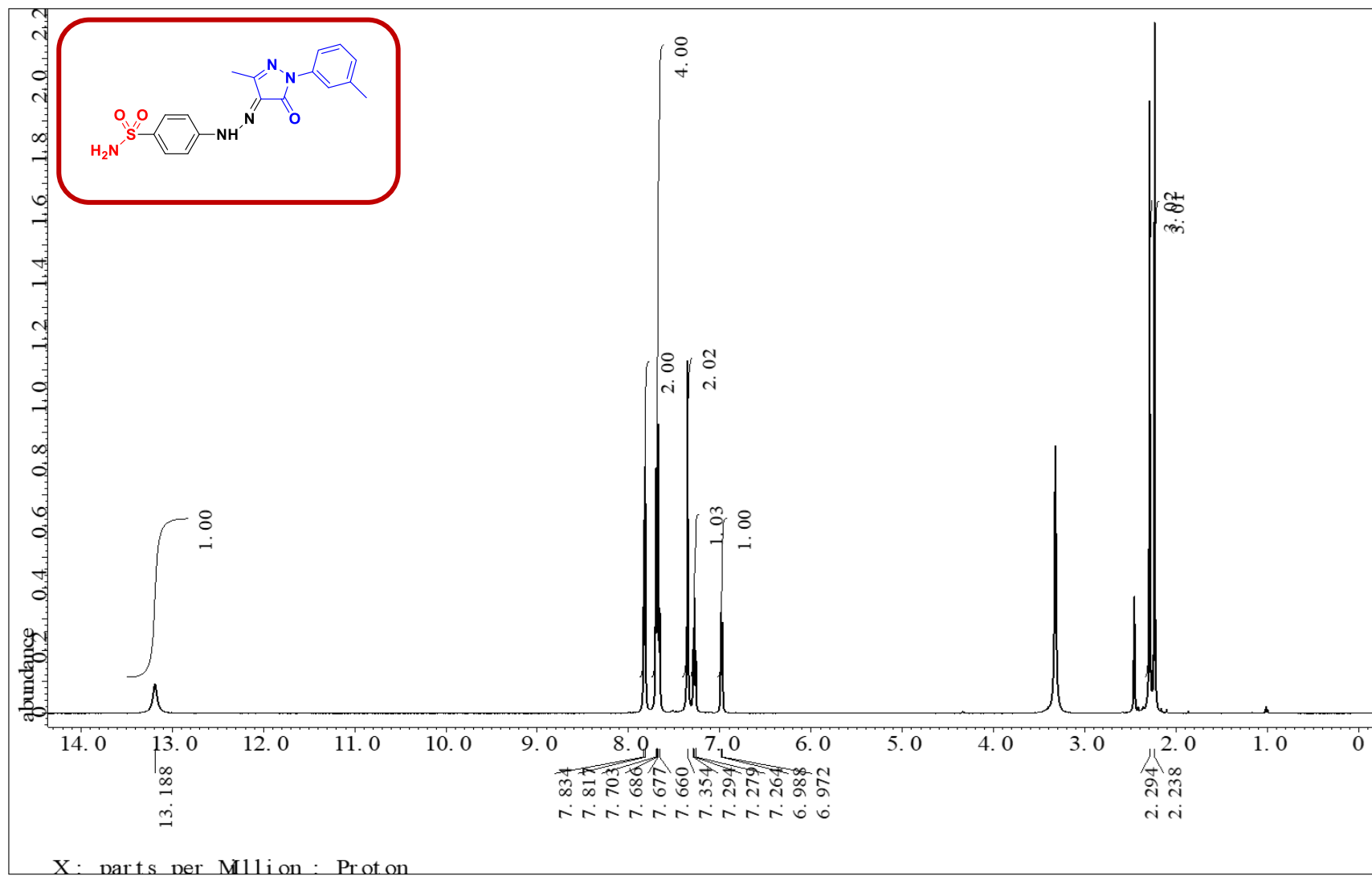


Fig. 19 $^1\text{H-NMR}$ spectrum (500 MHz, DMSO-d_6) of **3f**.

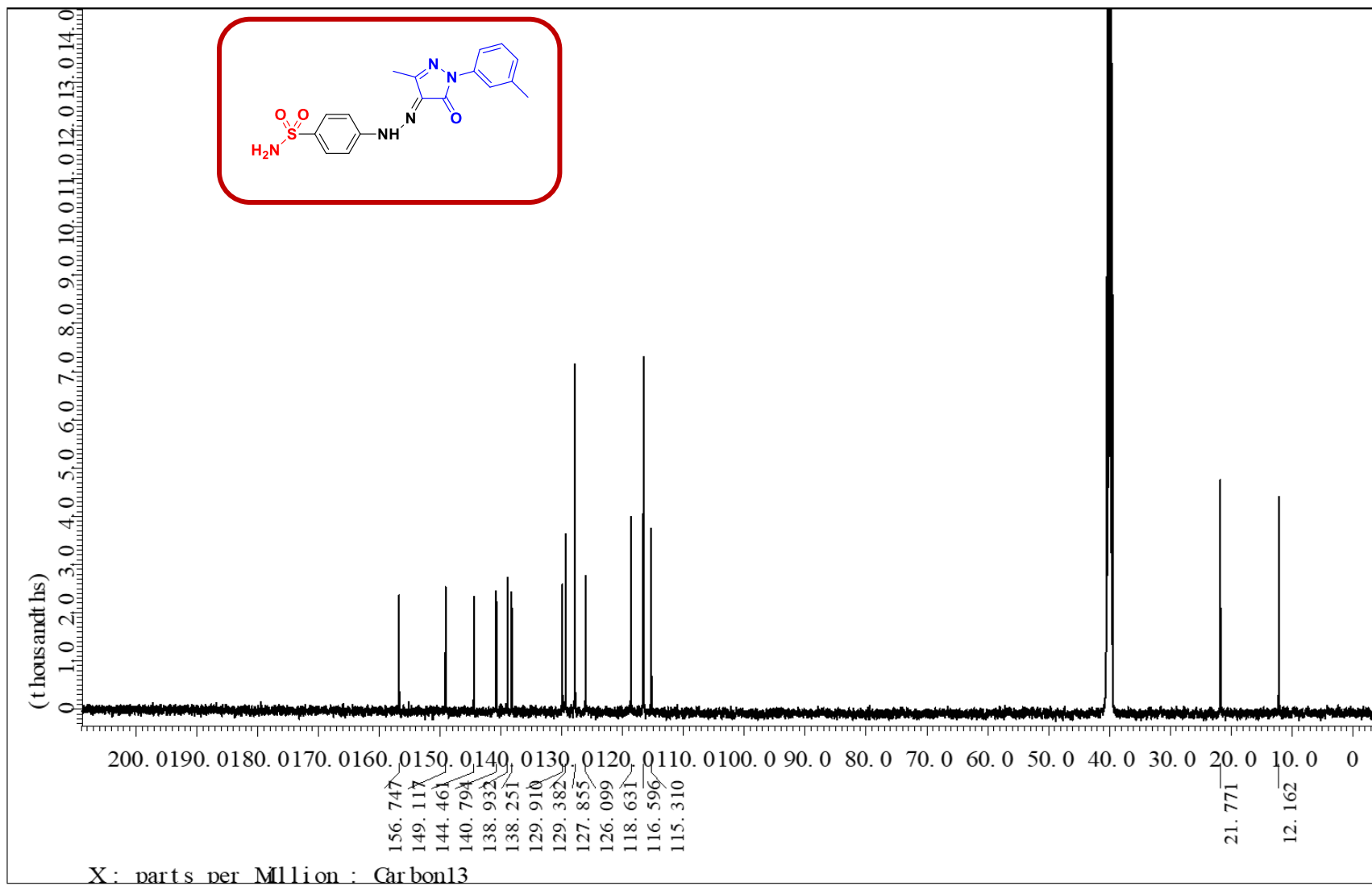


Fig. 20 ^{13}C -NMR spectrum (125 MHz, DMSO- d_6) of **3f**.

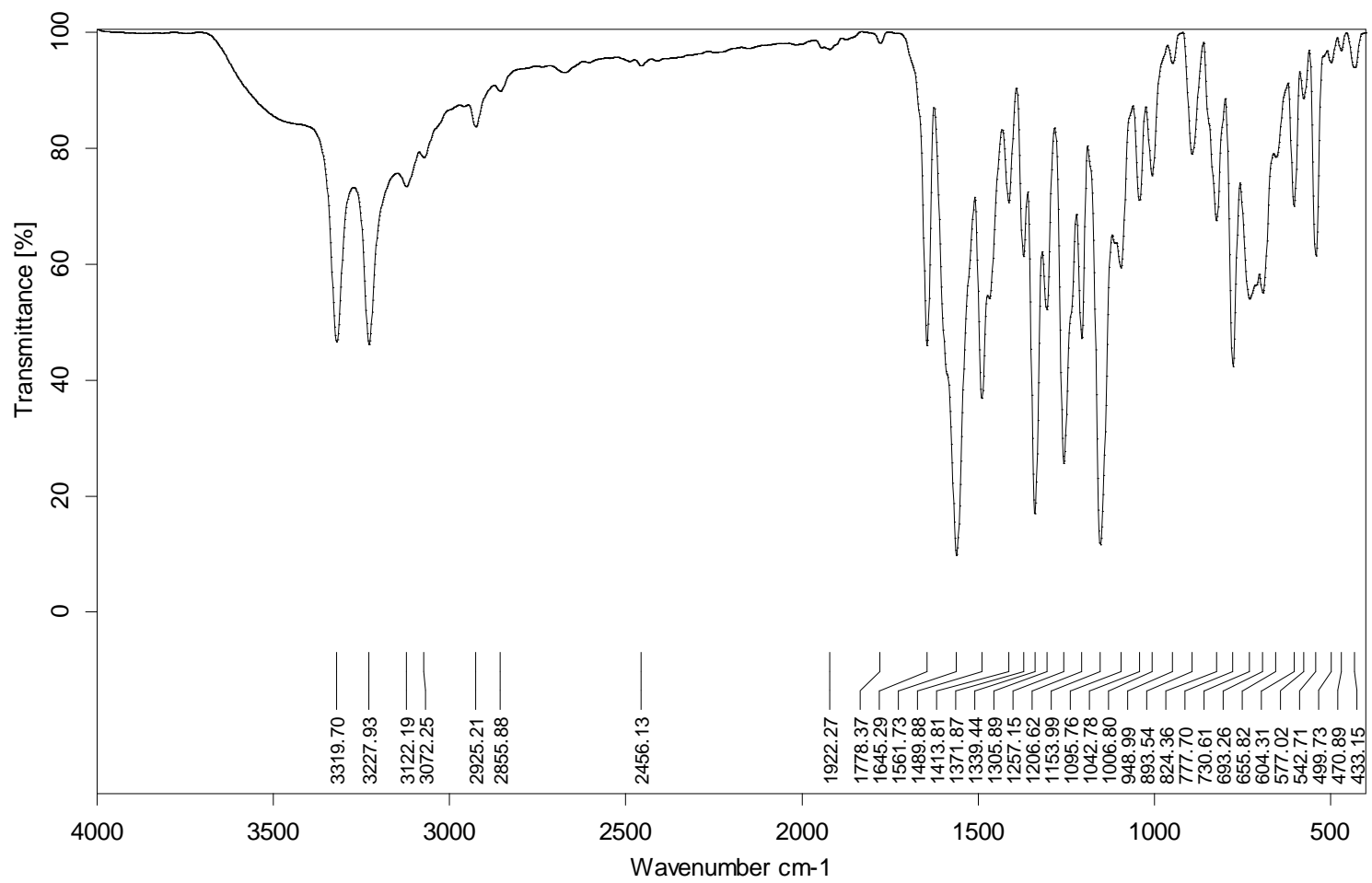


Fig. 21 IR spectrum of **3f**.

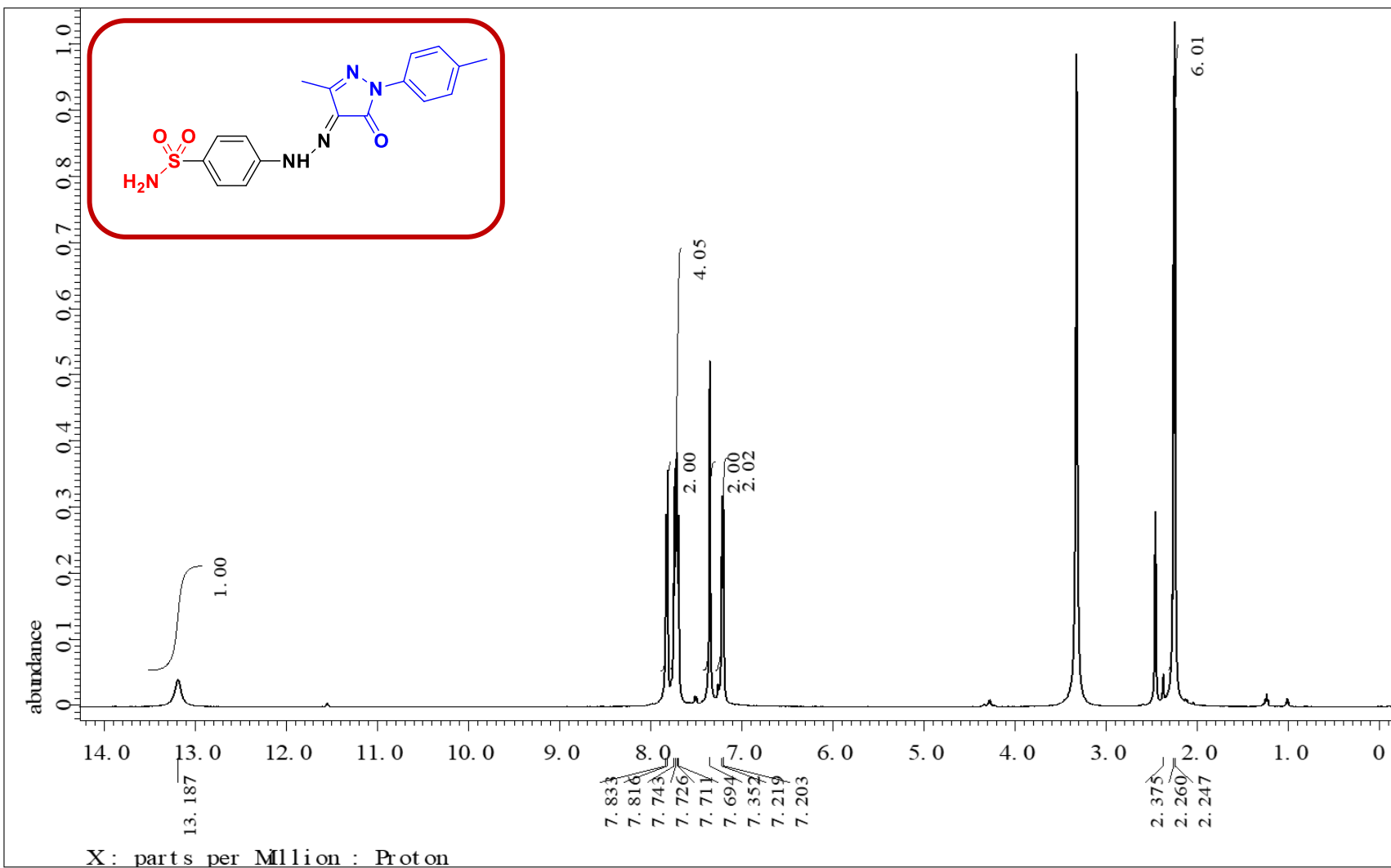


Fig. 22 ¹H-NMR spectrum (500 MHz, DMSO-d₆) of **3g**.

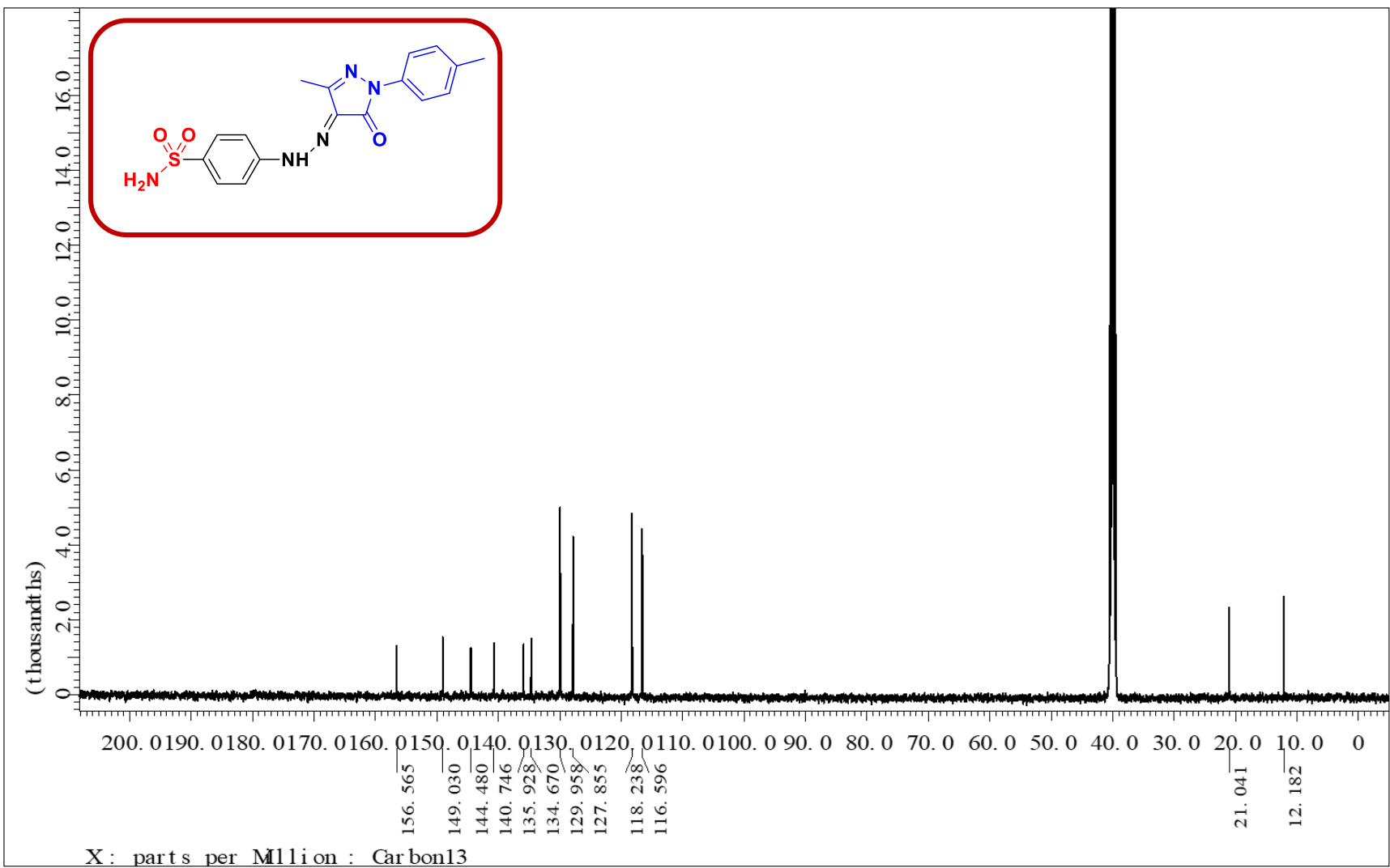


Fig. 23 $^{13}\text{C-NMR}$ spectrum (125 MHz, DMSO- d_6) of 3g.

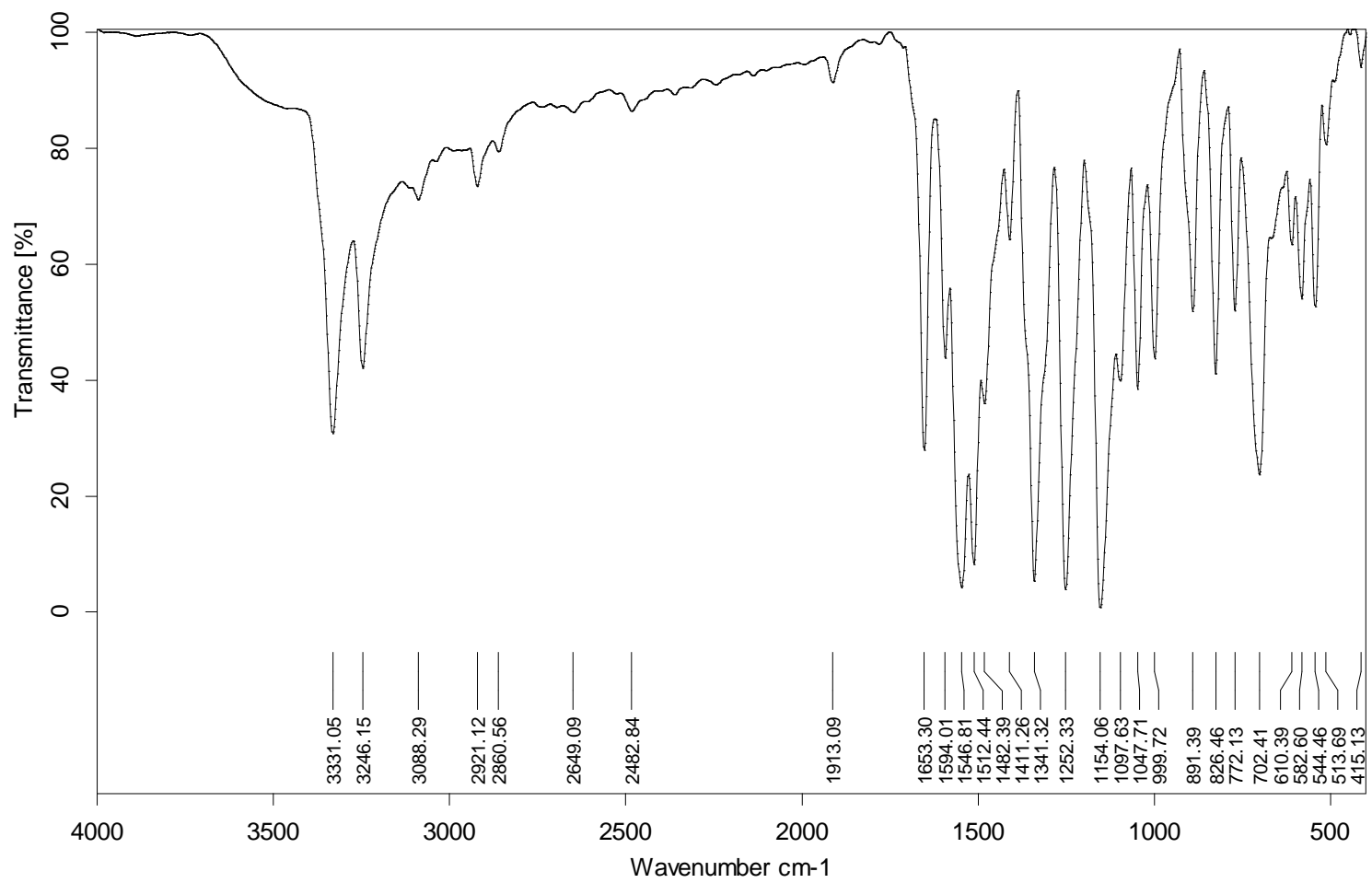


Fig. 24 IR spectrum of **3g**.

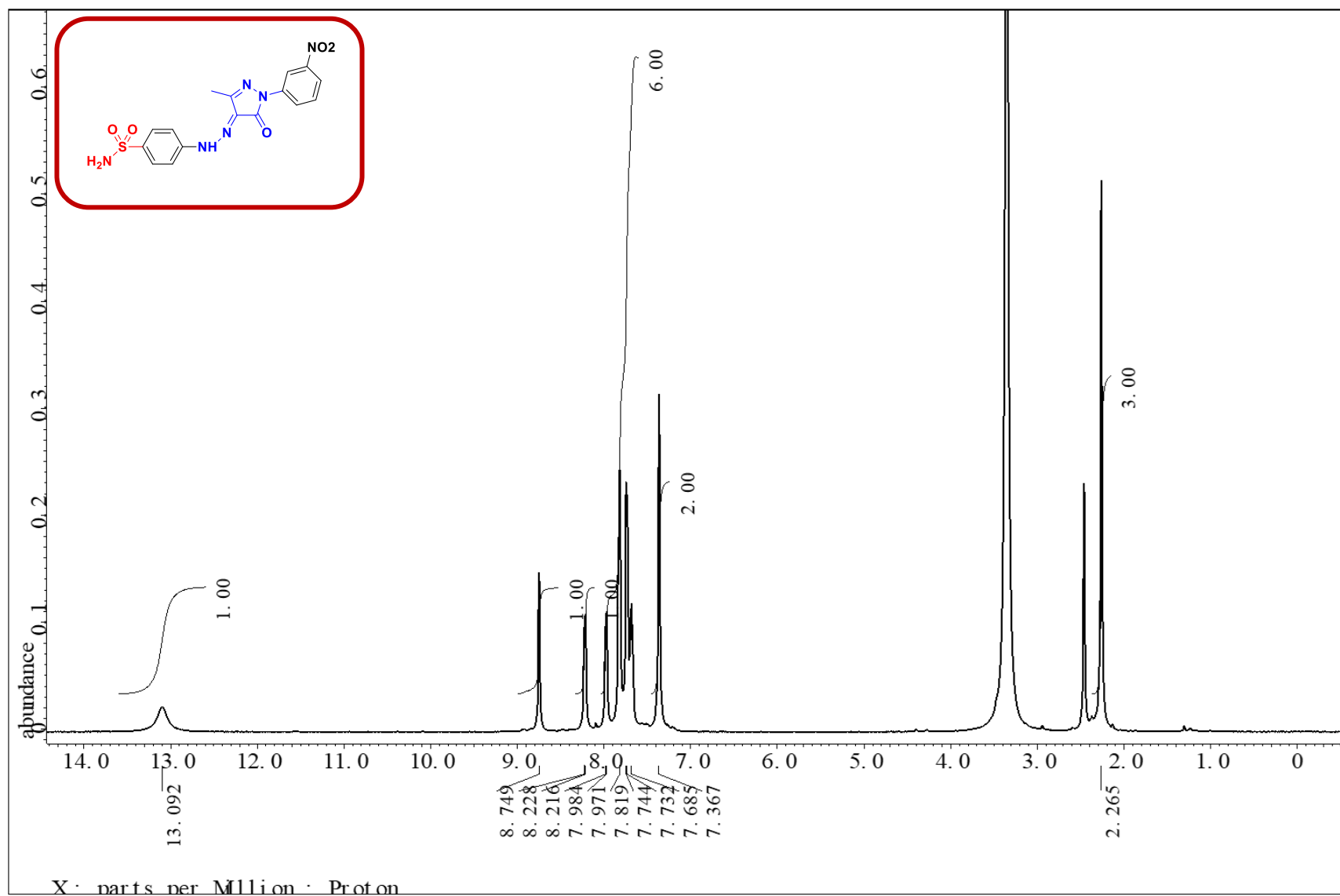


Fig. 25 ¹H-NMR spectrum (500 MHz, DMSO-d₆) of **3h**.

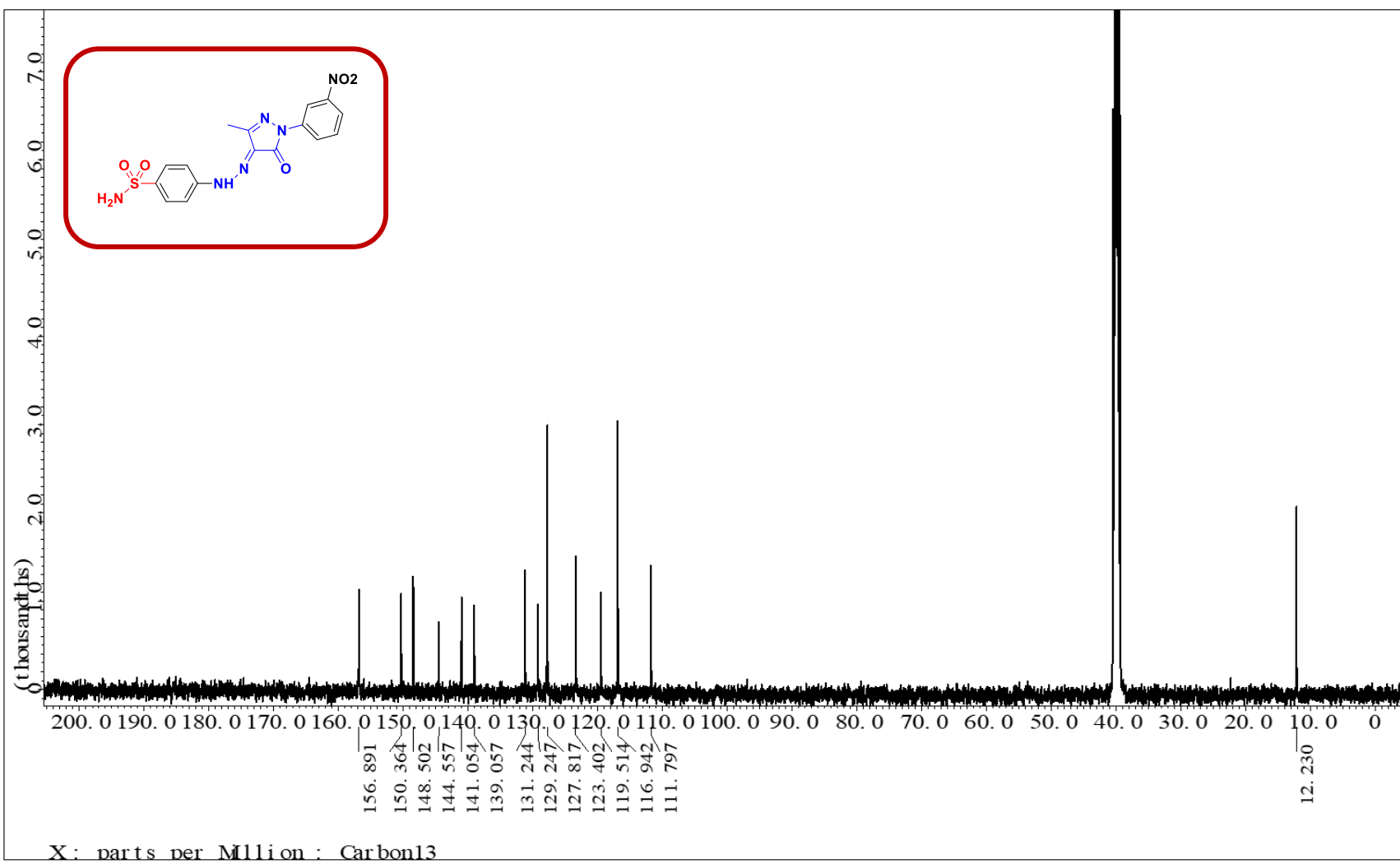


Fig. 26 ^{13}C -NMR spectrum (125 MHz, DMSO- d_6) of 3h.

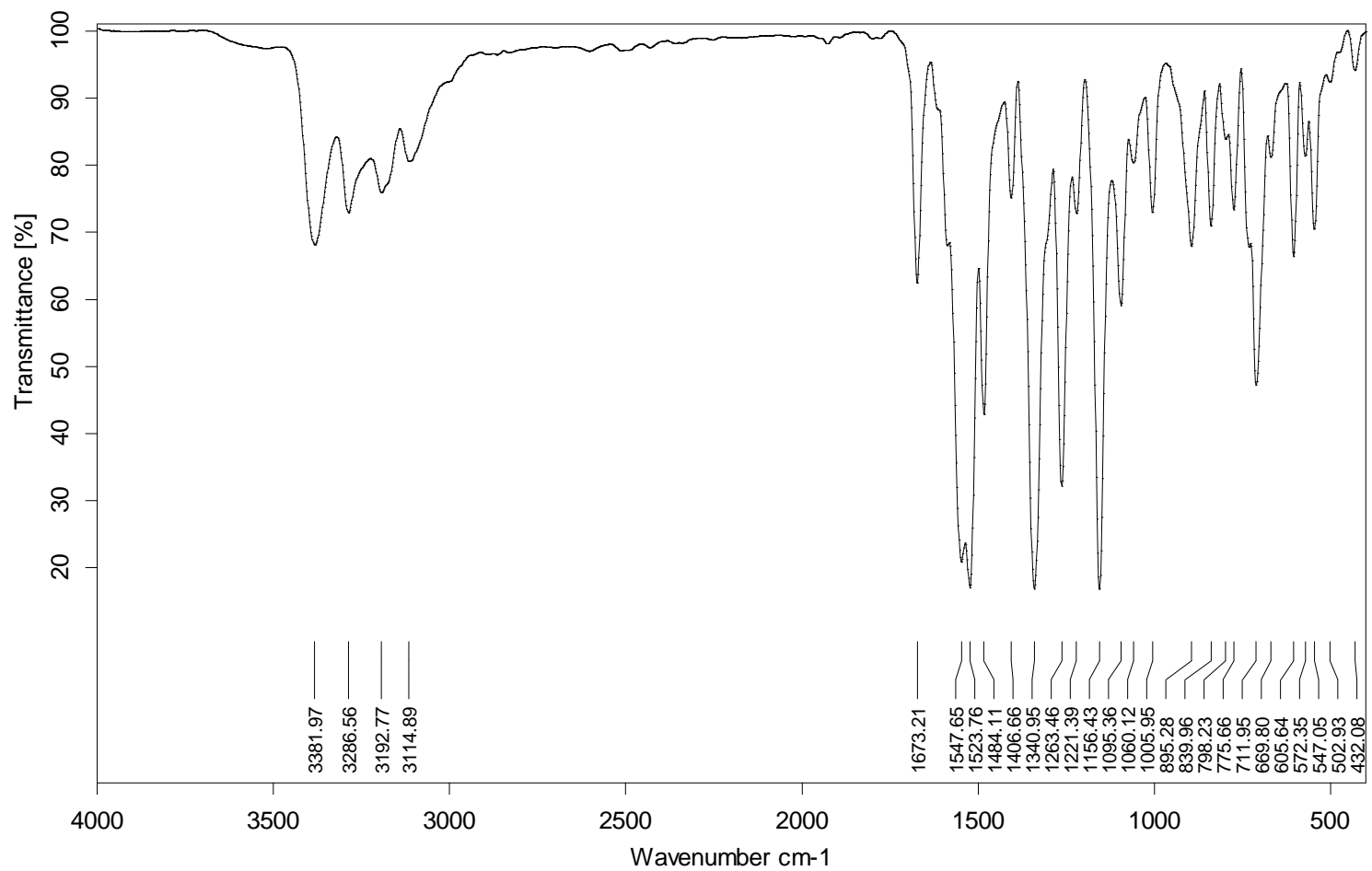


Fig. 27 IR spectrum of **3h**.

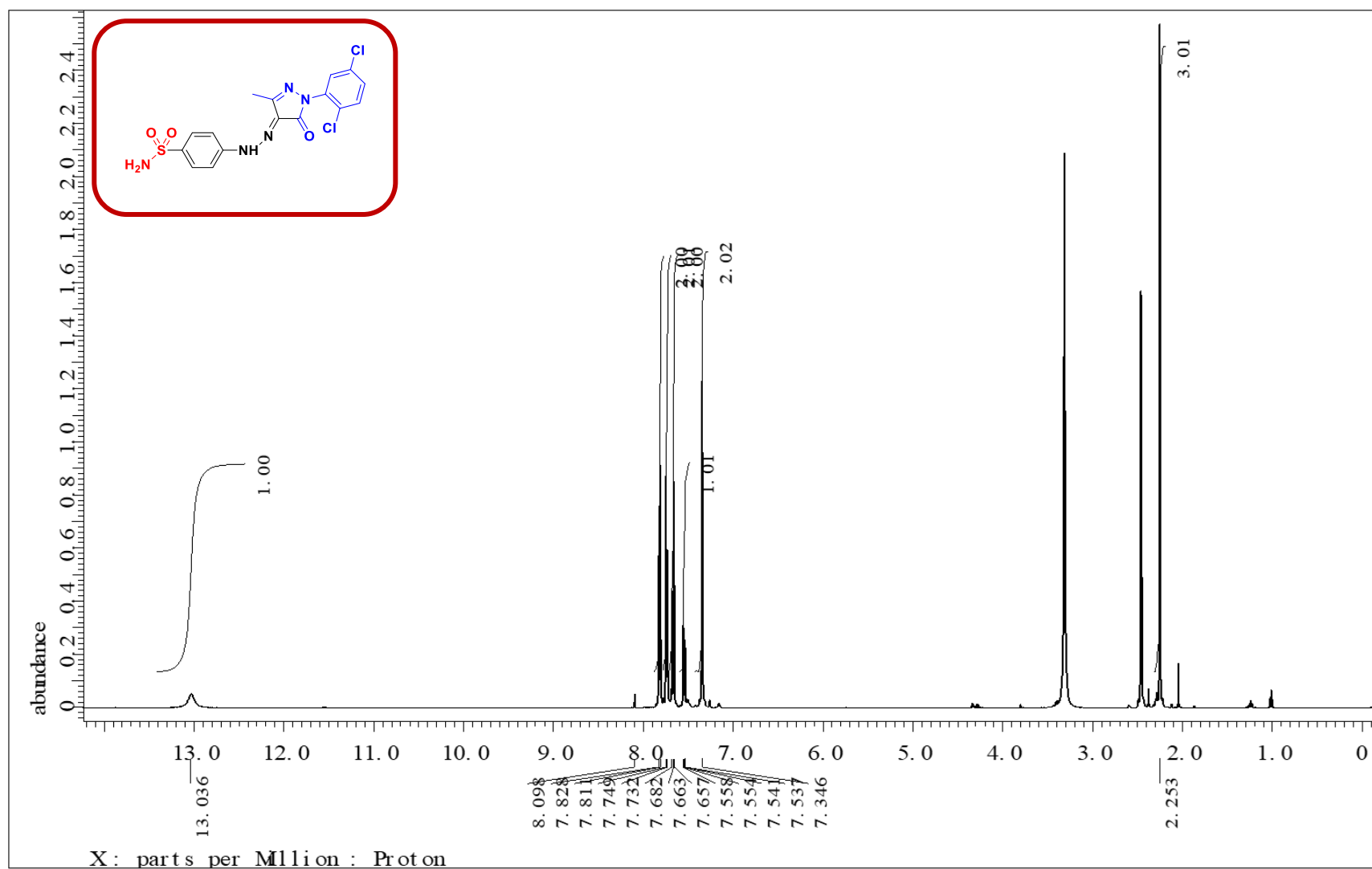


Fig. 28 ¹H-NMR spectrum (500 MHz, DMSO-d₆) of **3i**.

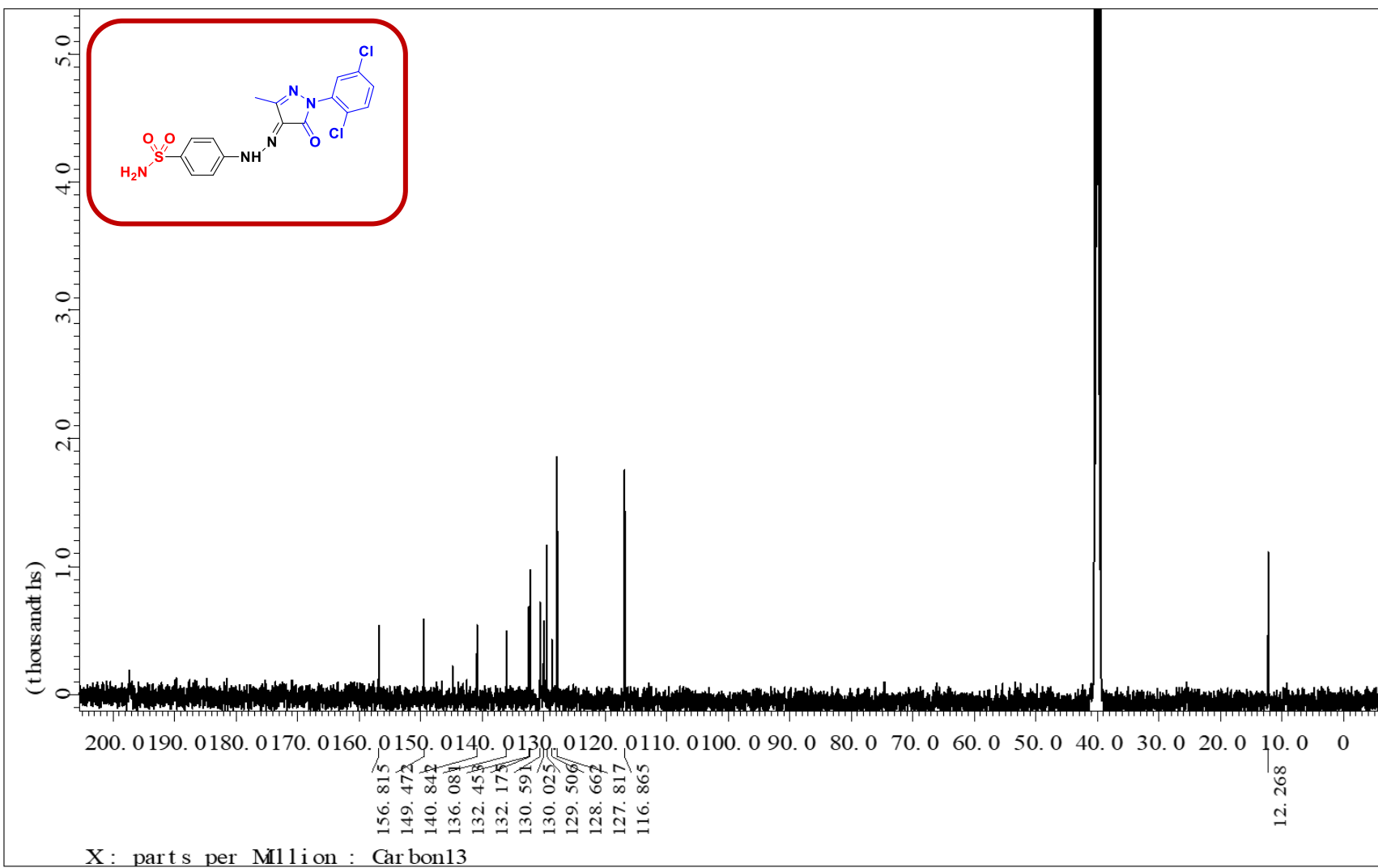


Fig. 29 ^{13}C -NMR spectrum (125 MHz, DMSO- d_6) of **3i**.

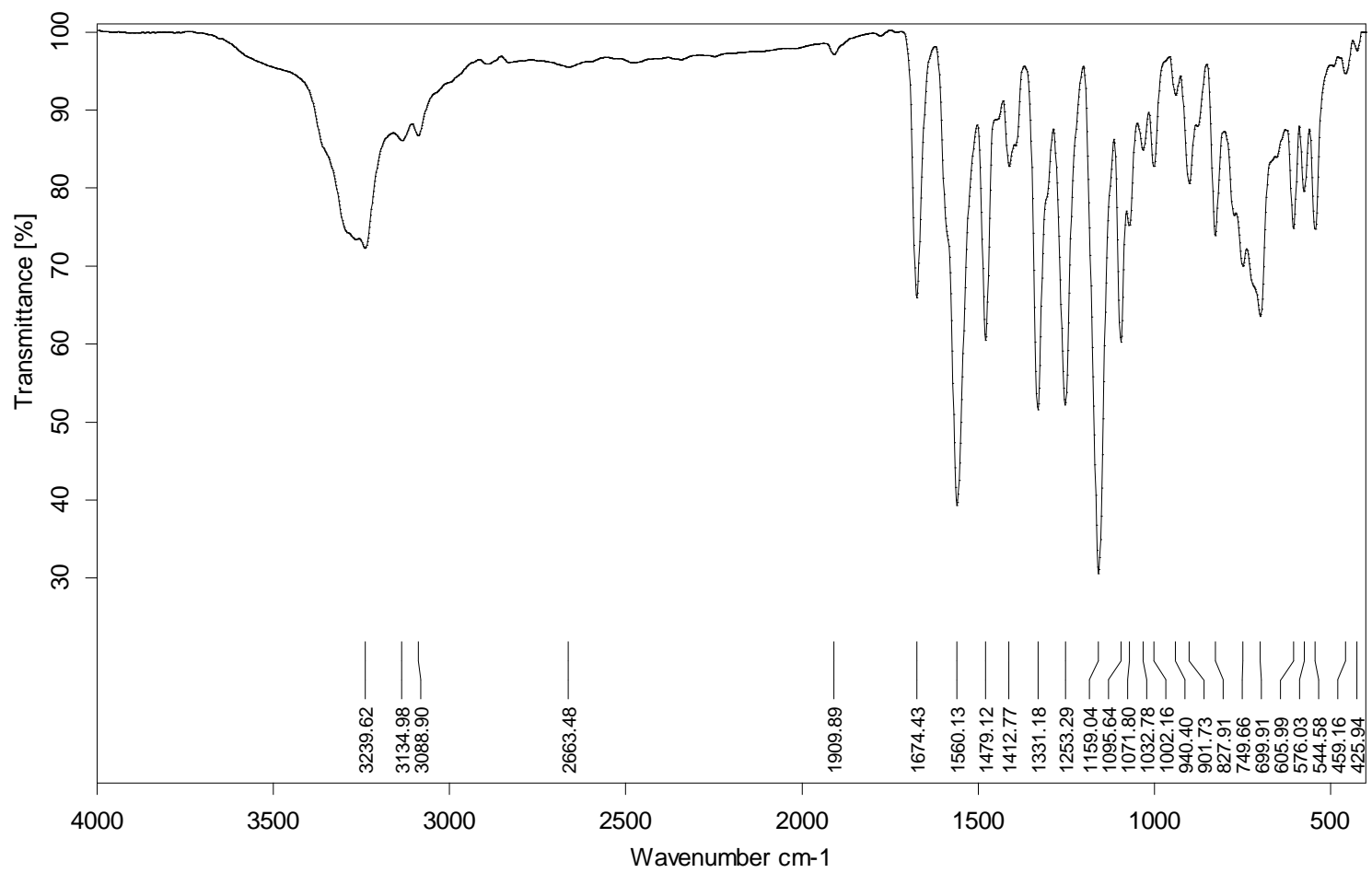


Fig. 30 IR spectrum of **3i**.

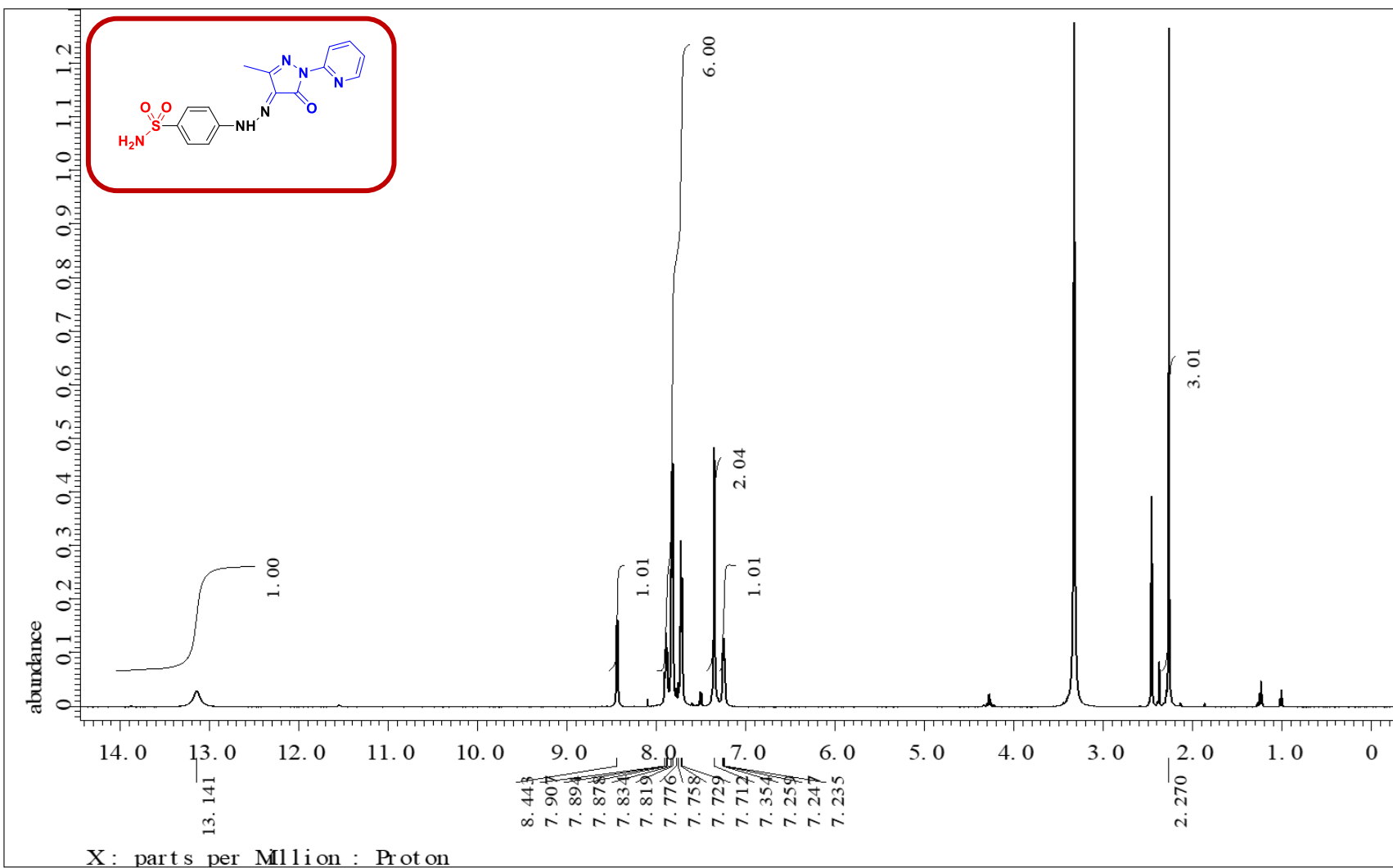


Fig. 31 ¹H-NMR spectrum (500 MHz, DMSO-d₆) of **3j**.

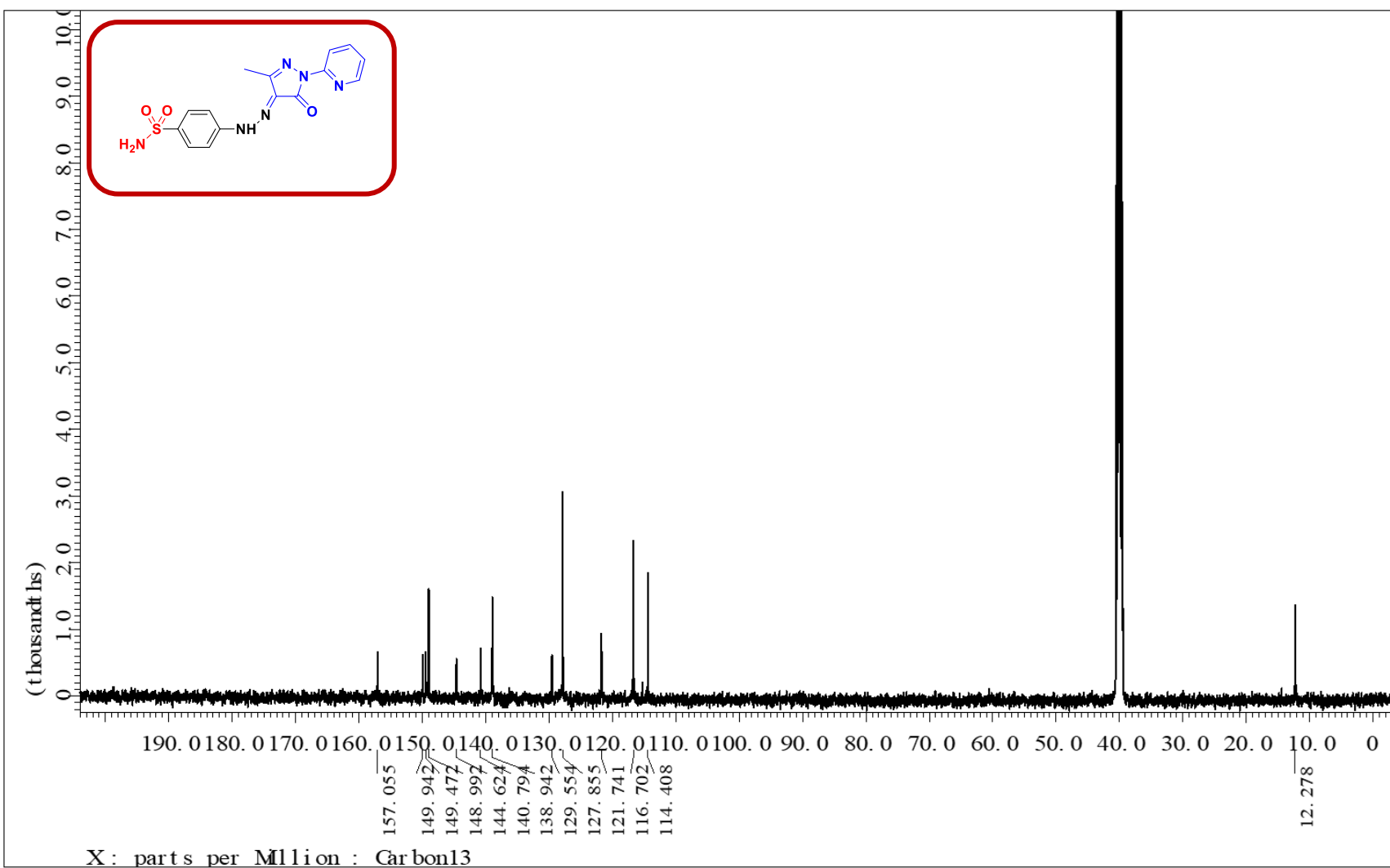


Fig. 32 ^{13}C -NMR spectrum (125 MHz, DMSO- d_6) of 3j.

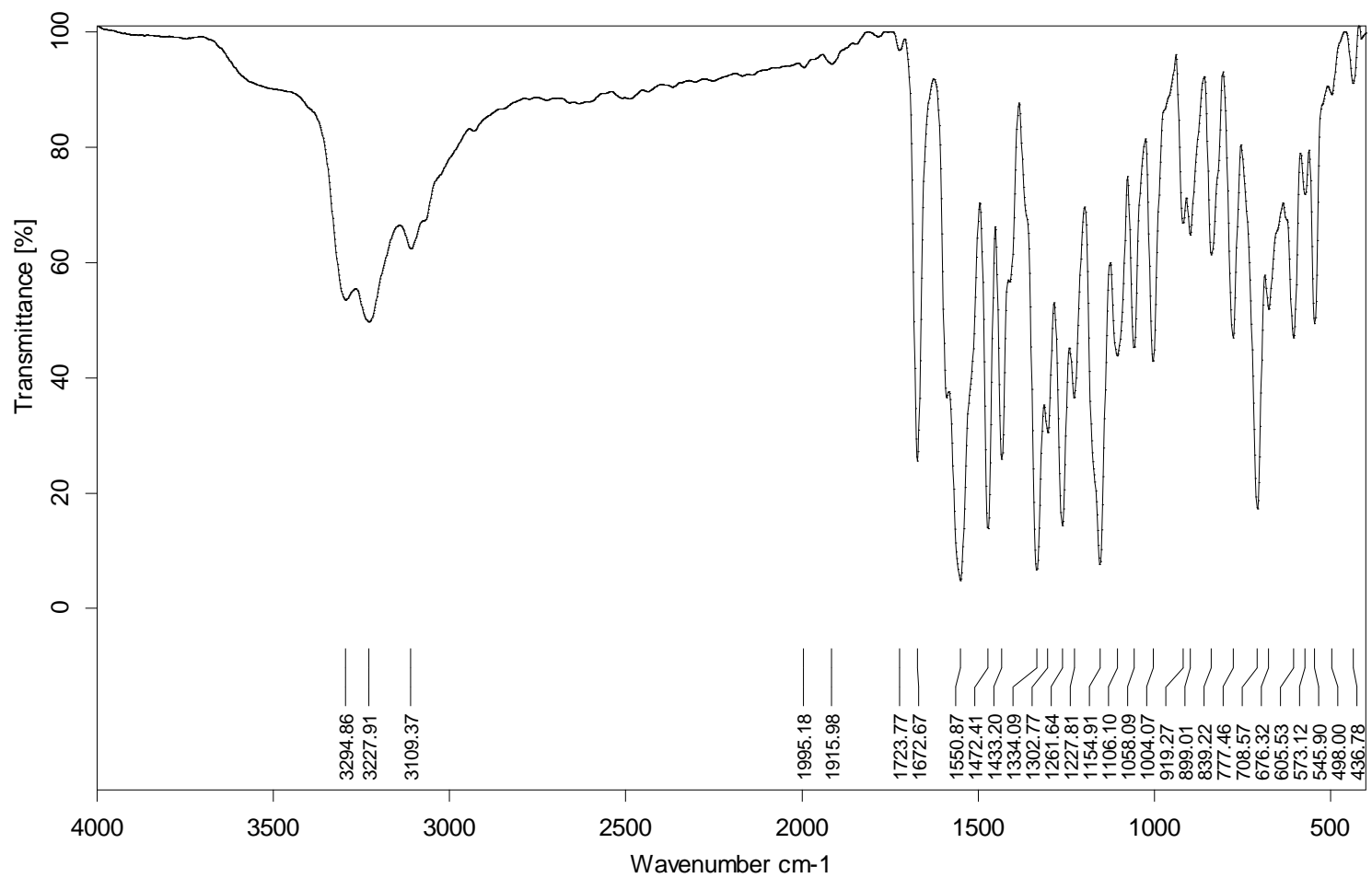


Fig. 33 IR spectrum of **3j**.

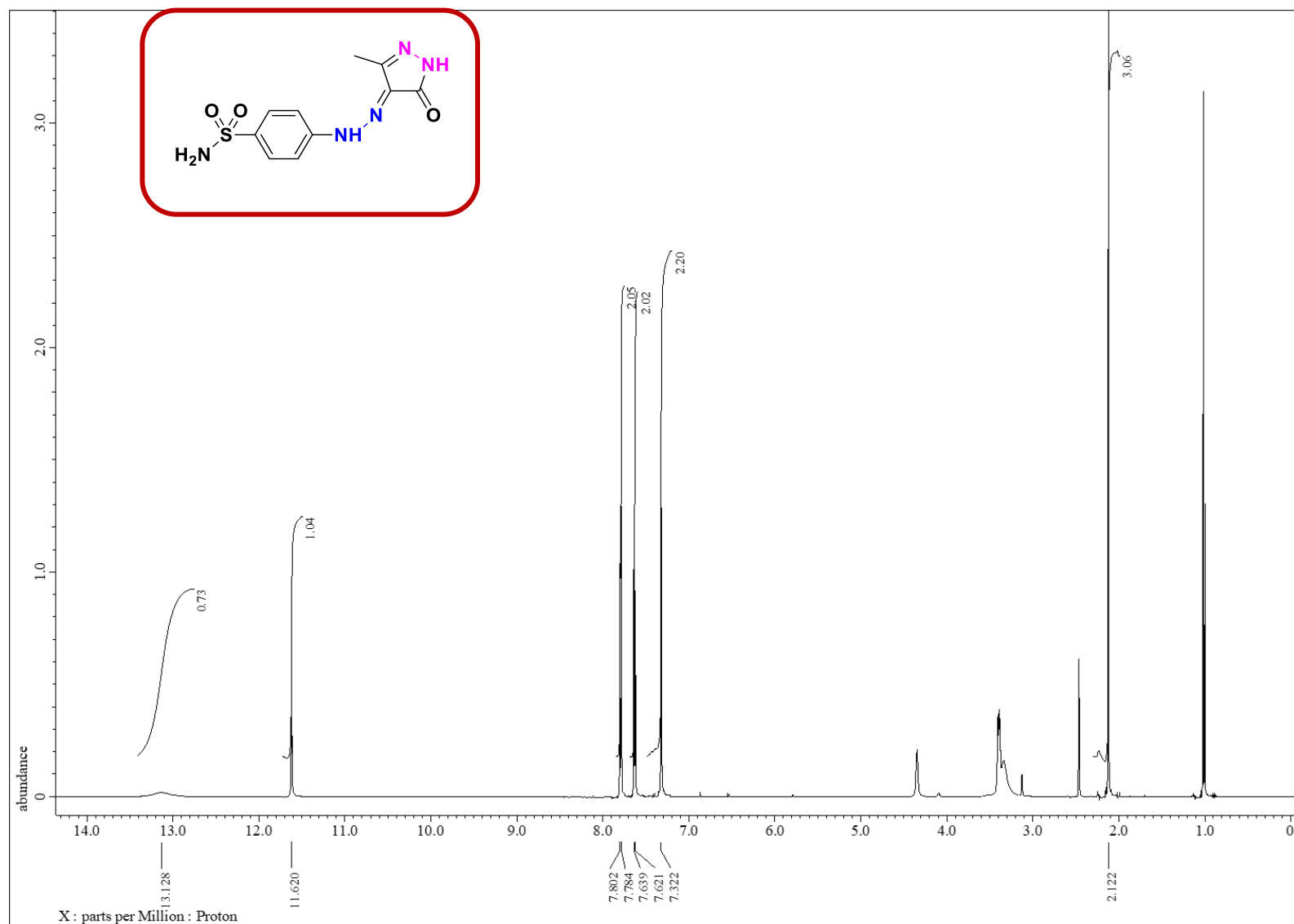


Fig. 34 ¹H-NMR spectrum (500 MHz, DMSO-d₆) of **4**.

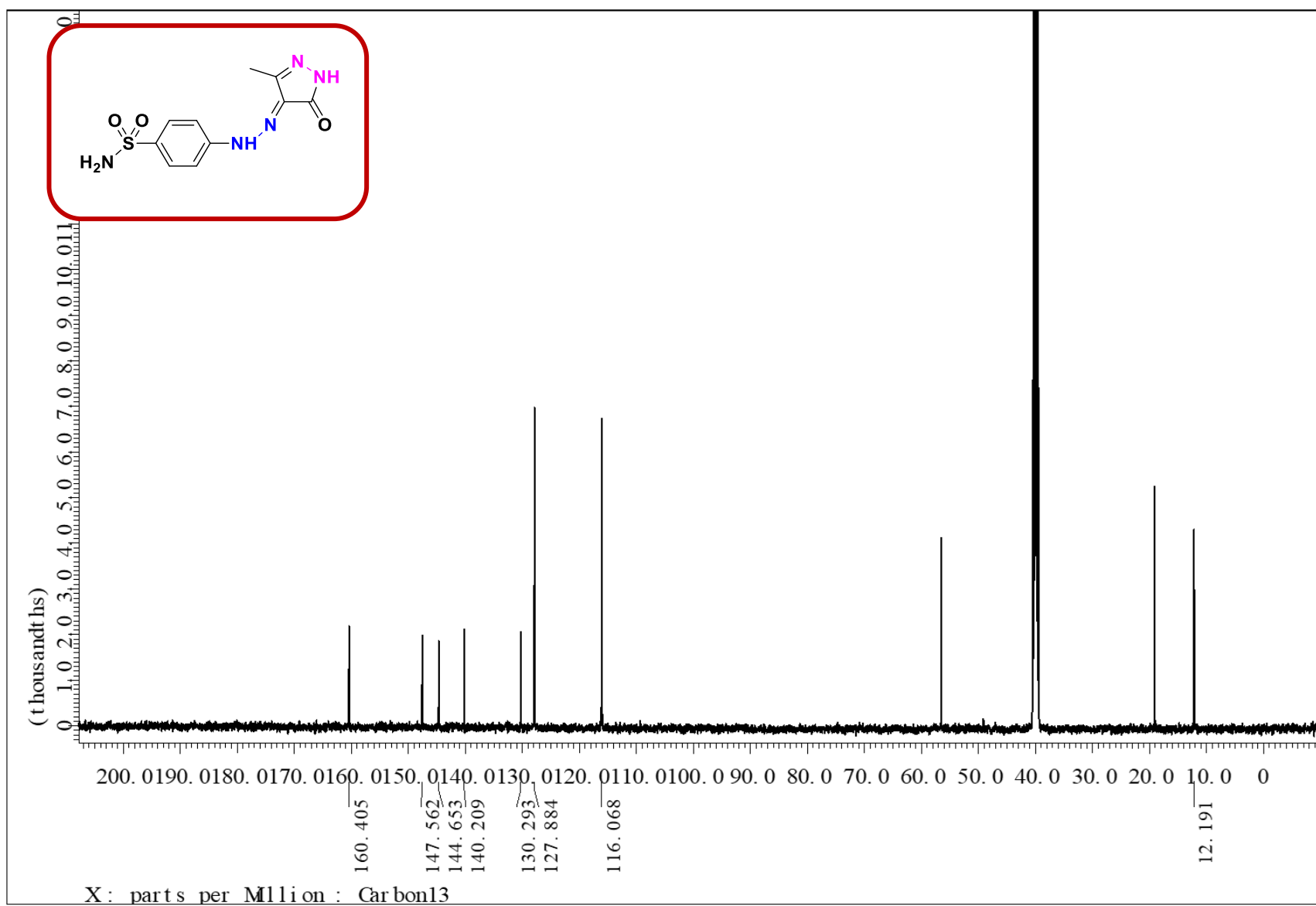


Fig. 35 $^{13}\text{C-NMR}$ spectrum (125 MHz, DMSO- d_6) of 4.

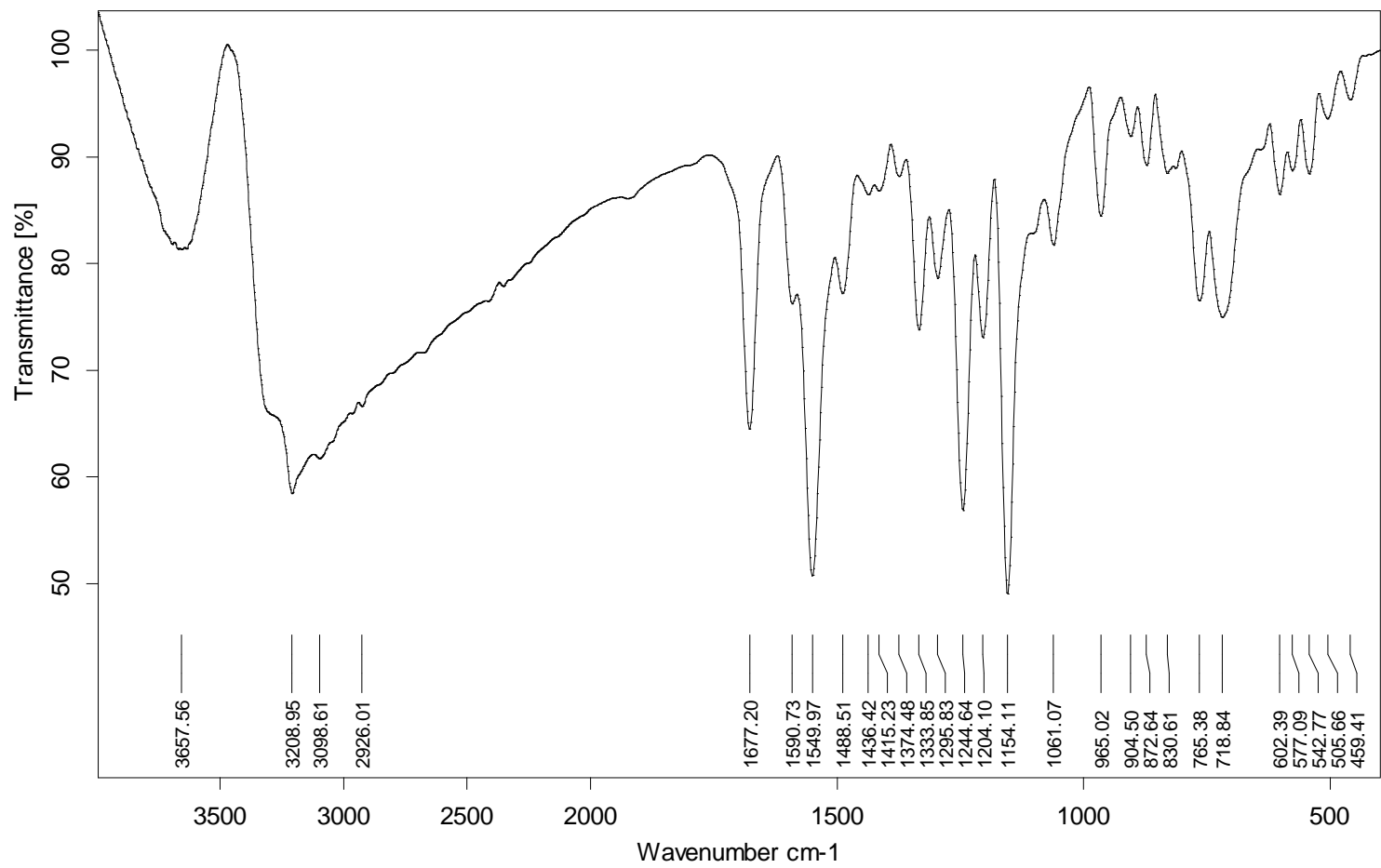


Fig. 36 IR spectrum of **4**.

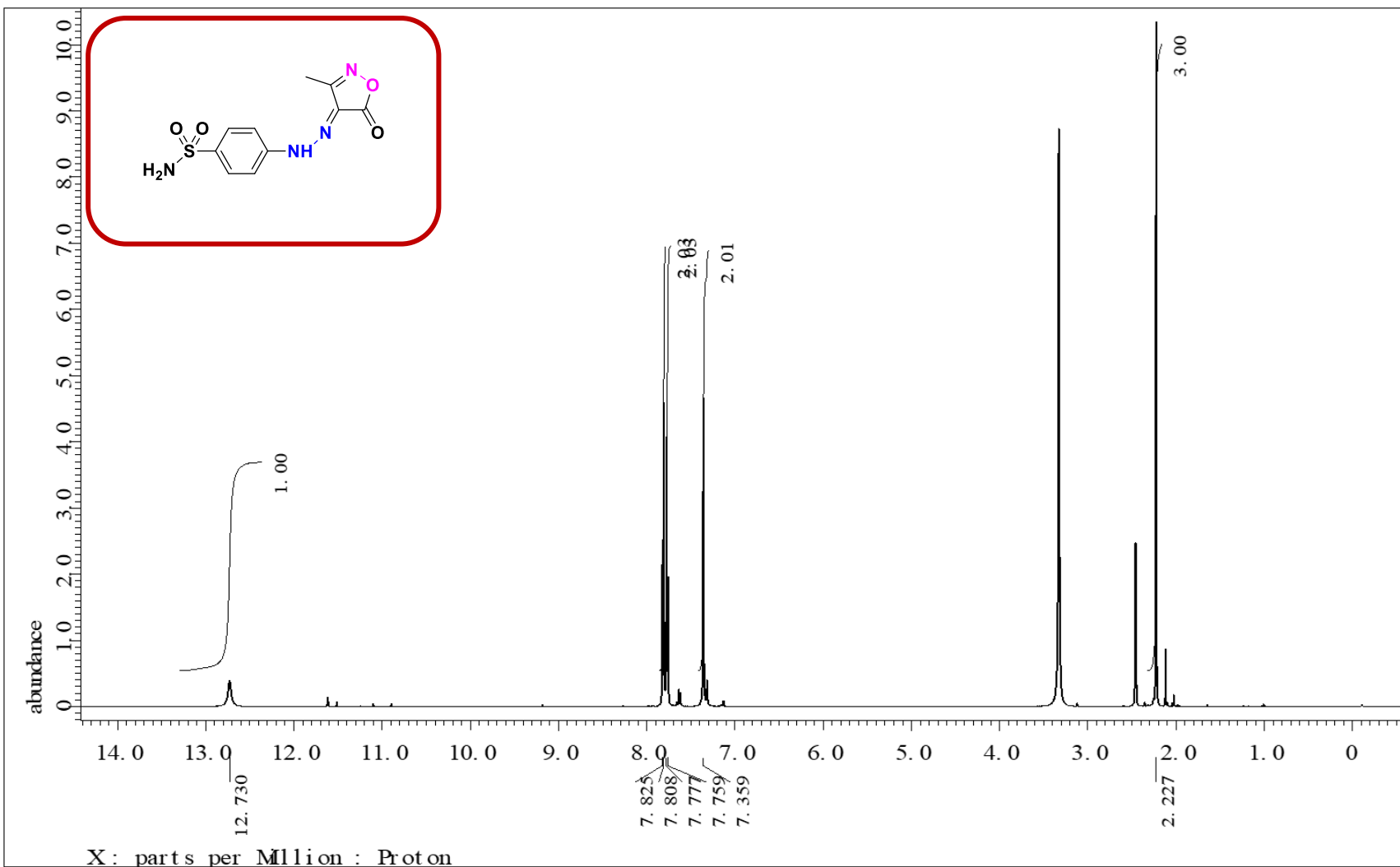


Fig. 37 $^1\text{H-NMR}$ spectrum (500 MHz, DMSO-d_6) of **5**.

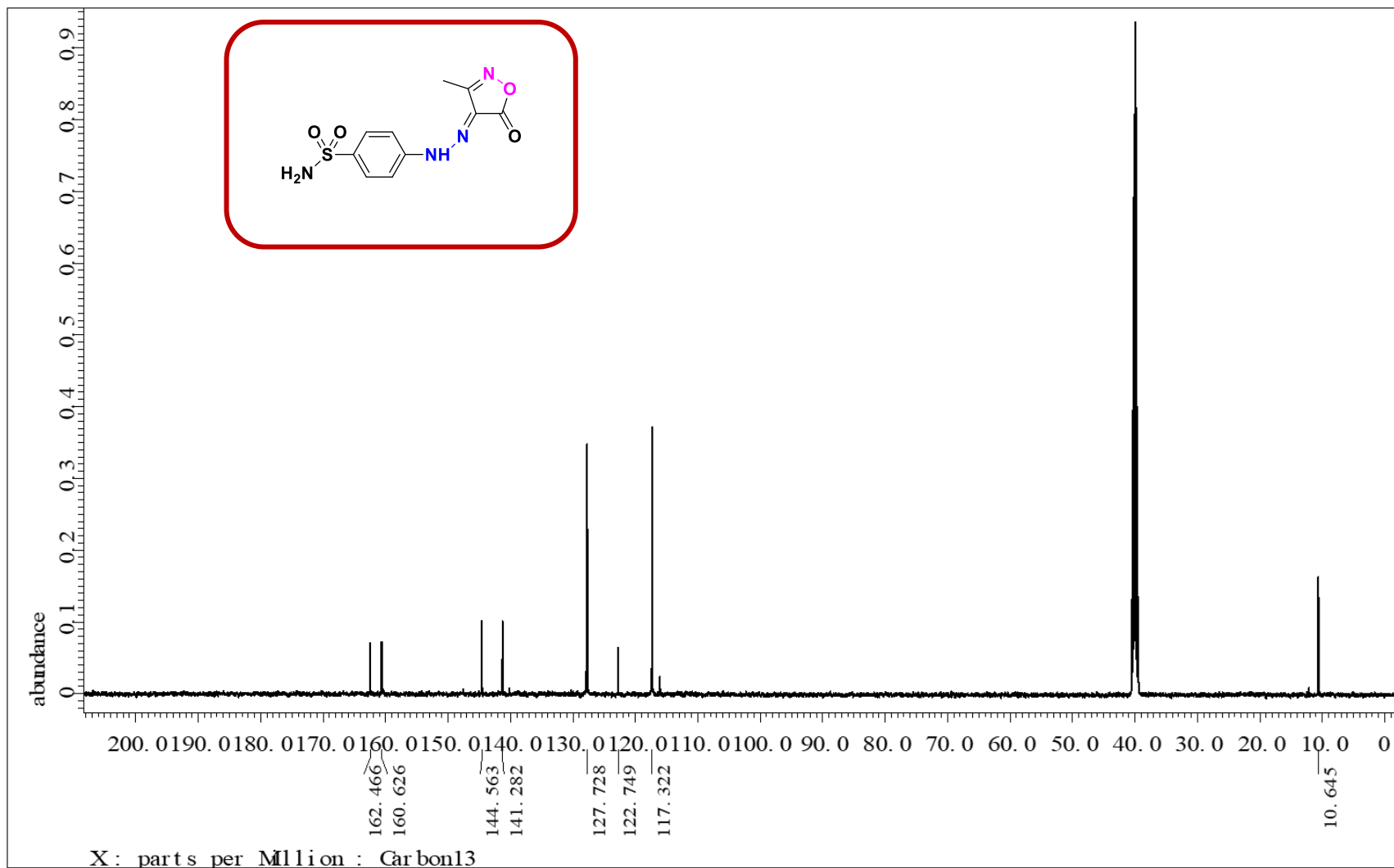


Fig. 38 ^{13}C -NMR spectrum (125 MHz, DMSO- d_6) of 5.

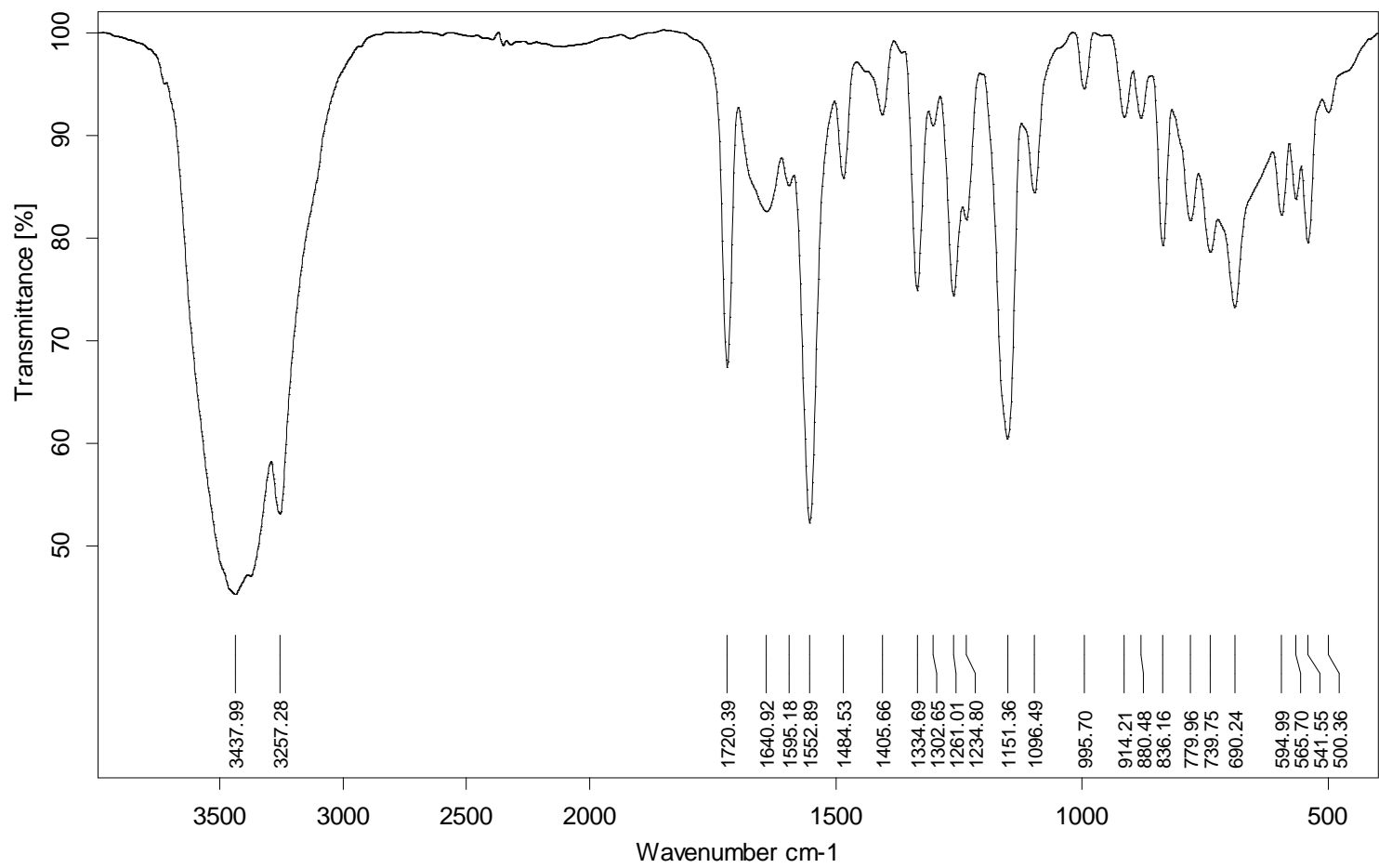


Fig. 39 IR spectrum of **5**.

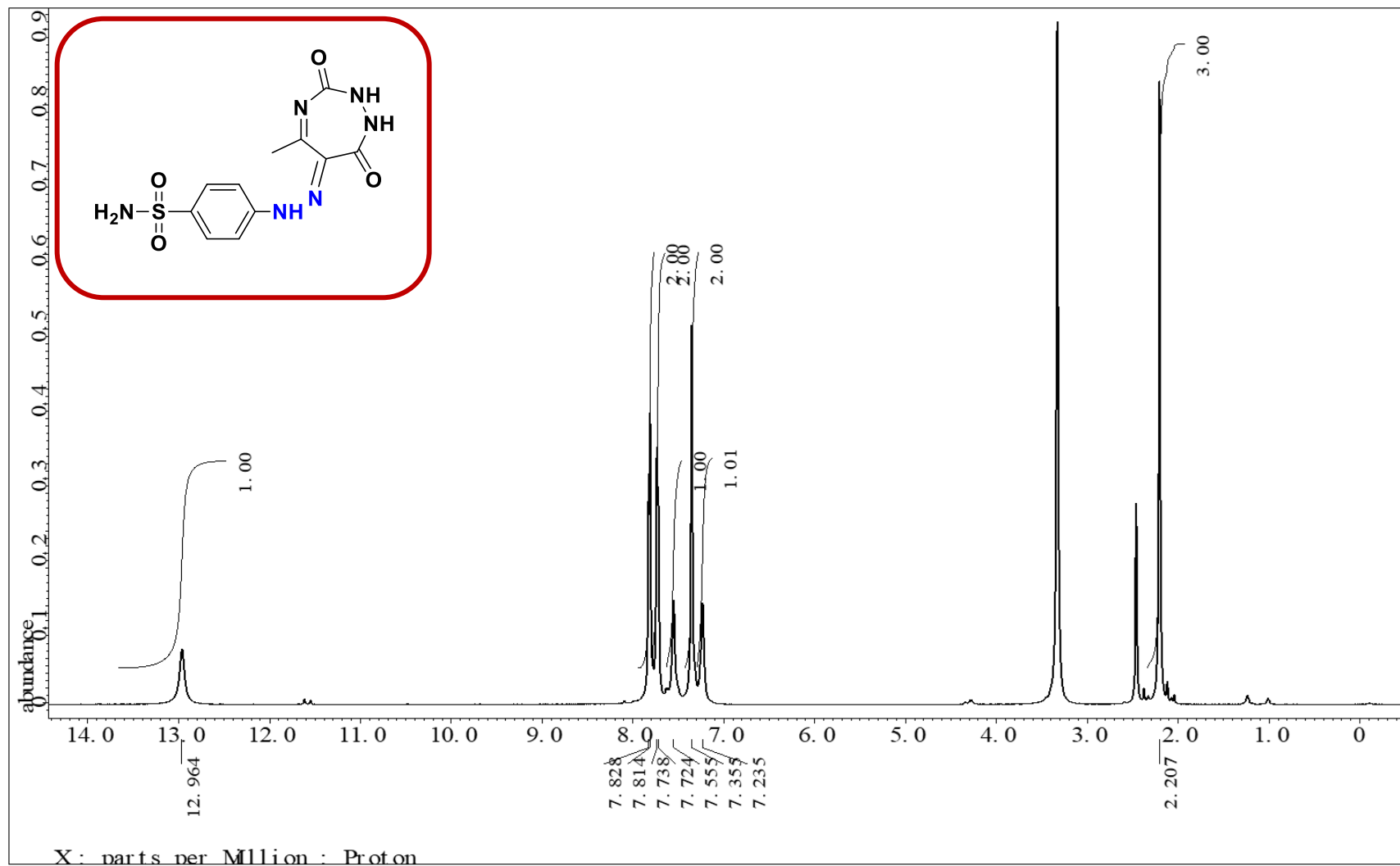


Fig. 40 $^1\text{H-NMR}$ spectrum (500 MHz, DMSO-d_6) of 6.

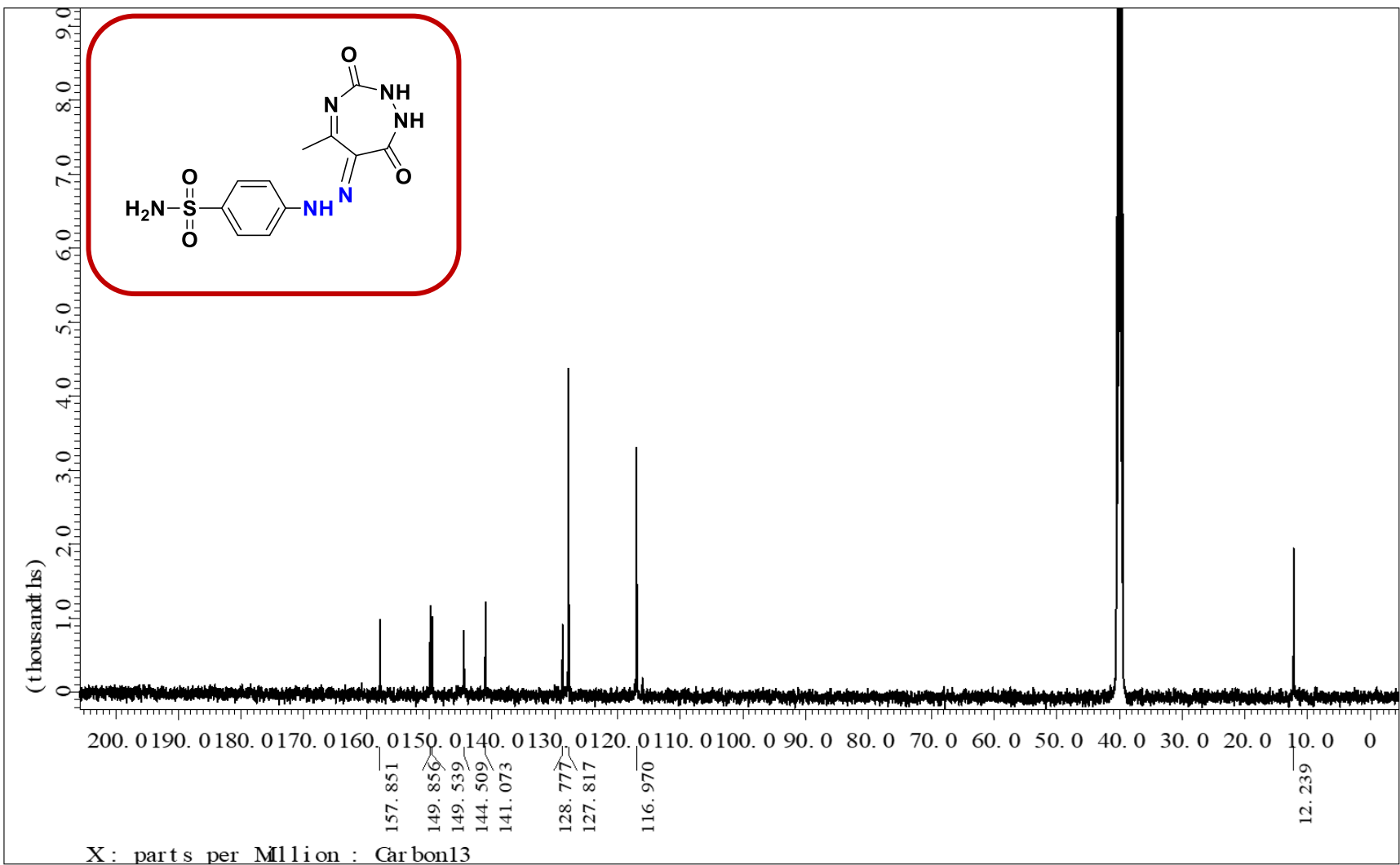


Fig. 41 $^{13}\text{C-NMR}$ spectrum (125 MHz, DMSO-d_6) of 6.

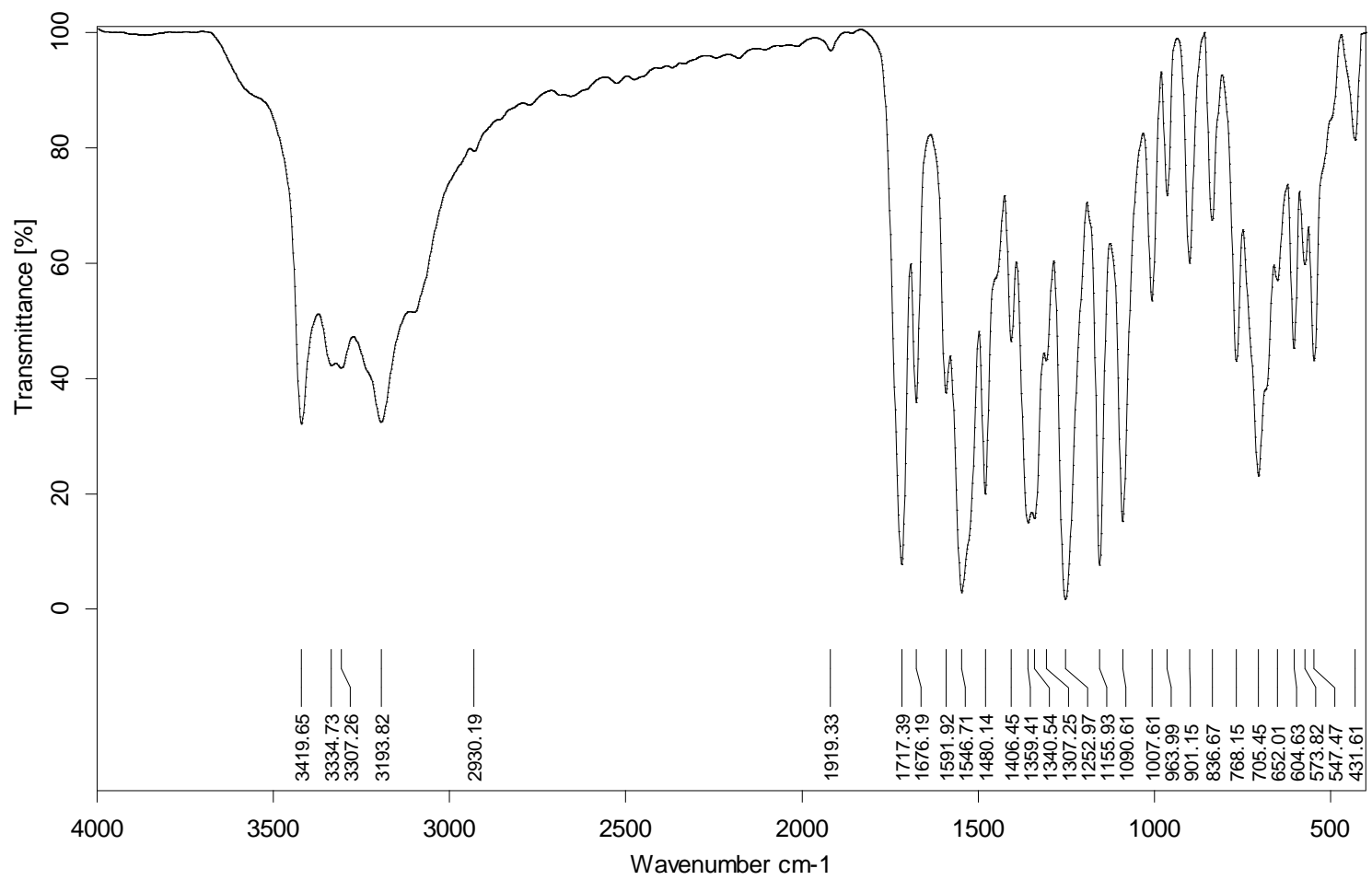


Fig. 42 IR spectrum of **6**.

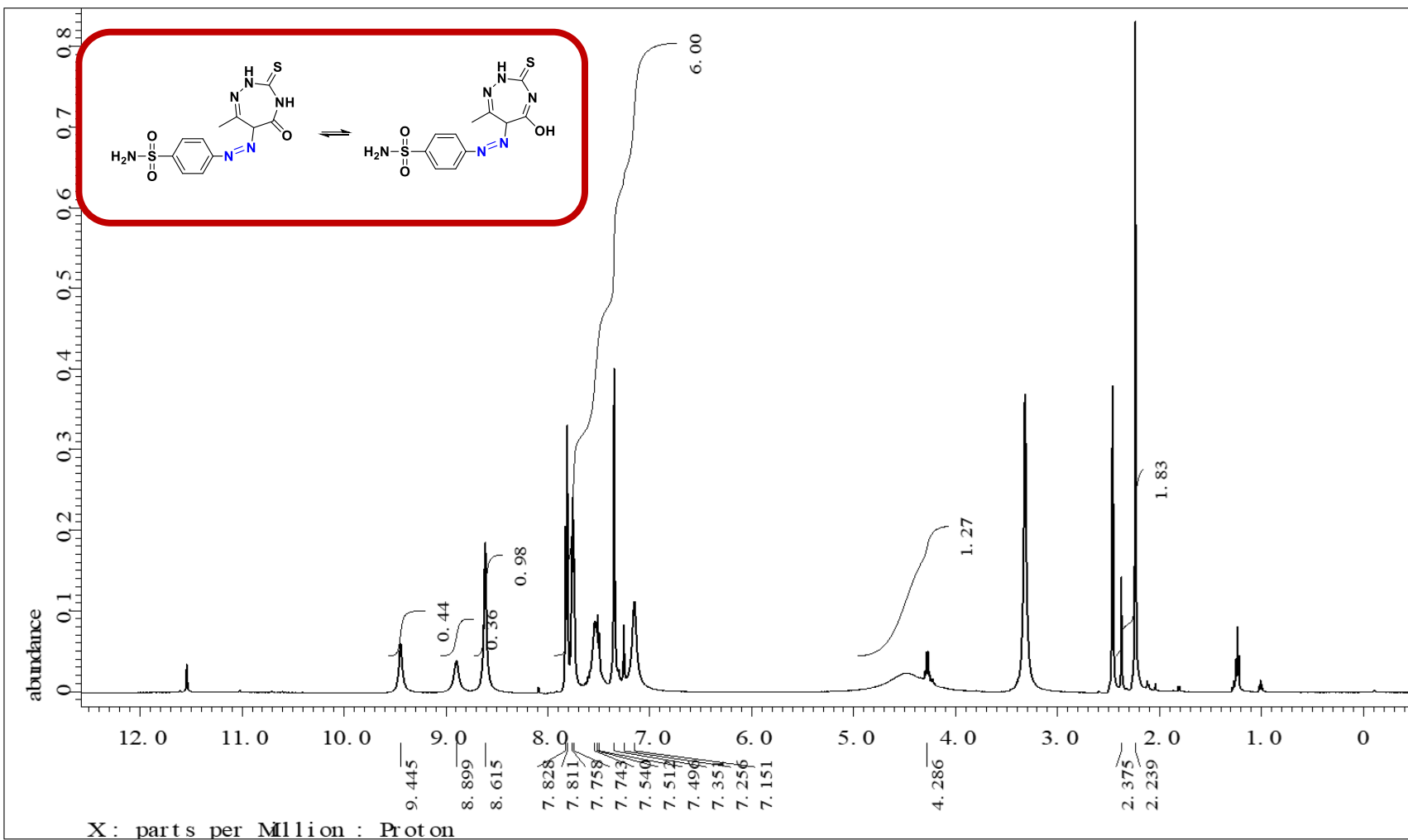


Fig. 43 $^1\text{H-NMR}$ spectrum (500 MHz, DMSO-d_6) of 7.

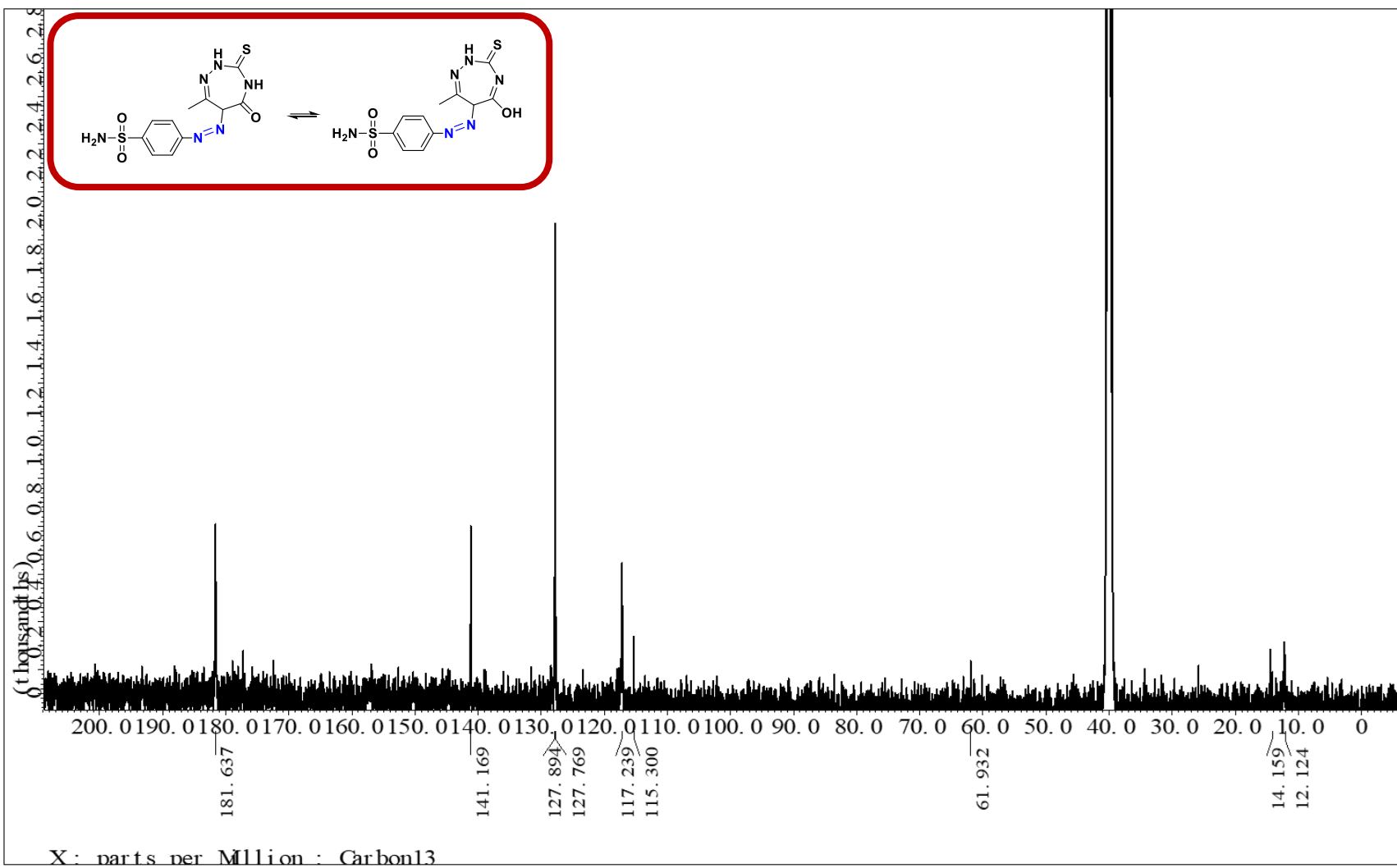


Fig. 44 $^{13}\text{C-NMR}$ spectrum (125 MHz, DMSO- d_6) of 7

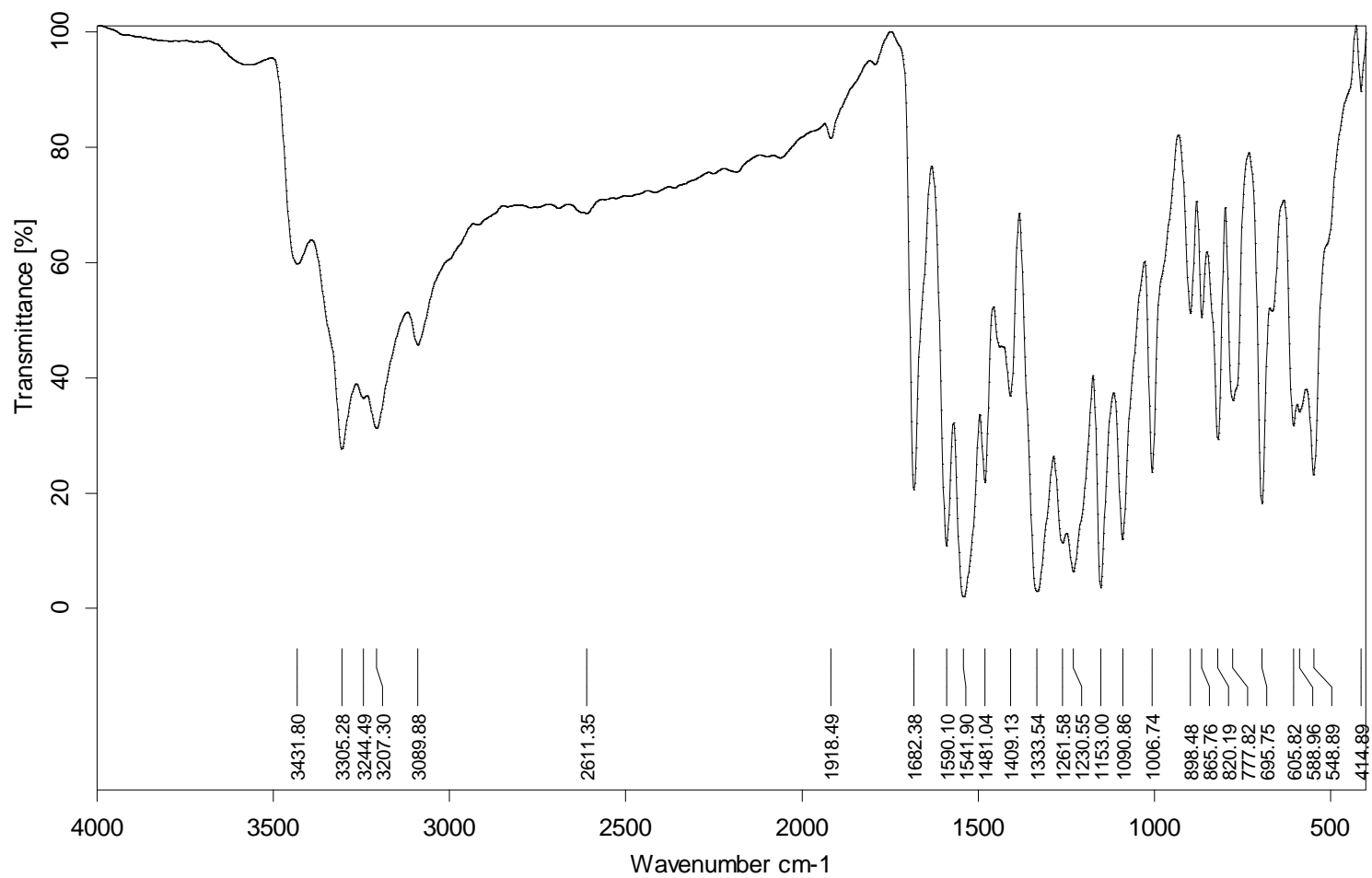


Fig. 45 IR spectrum of **7**.

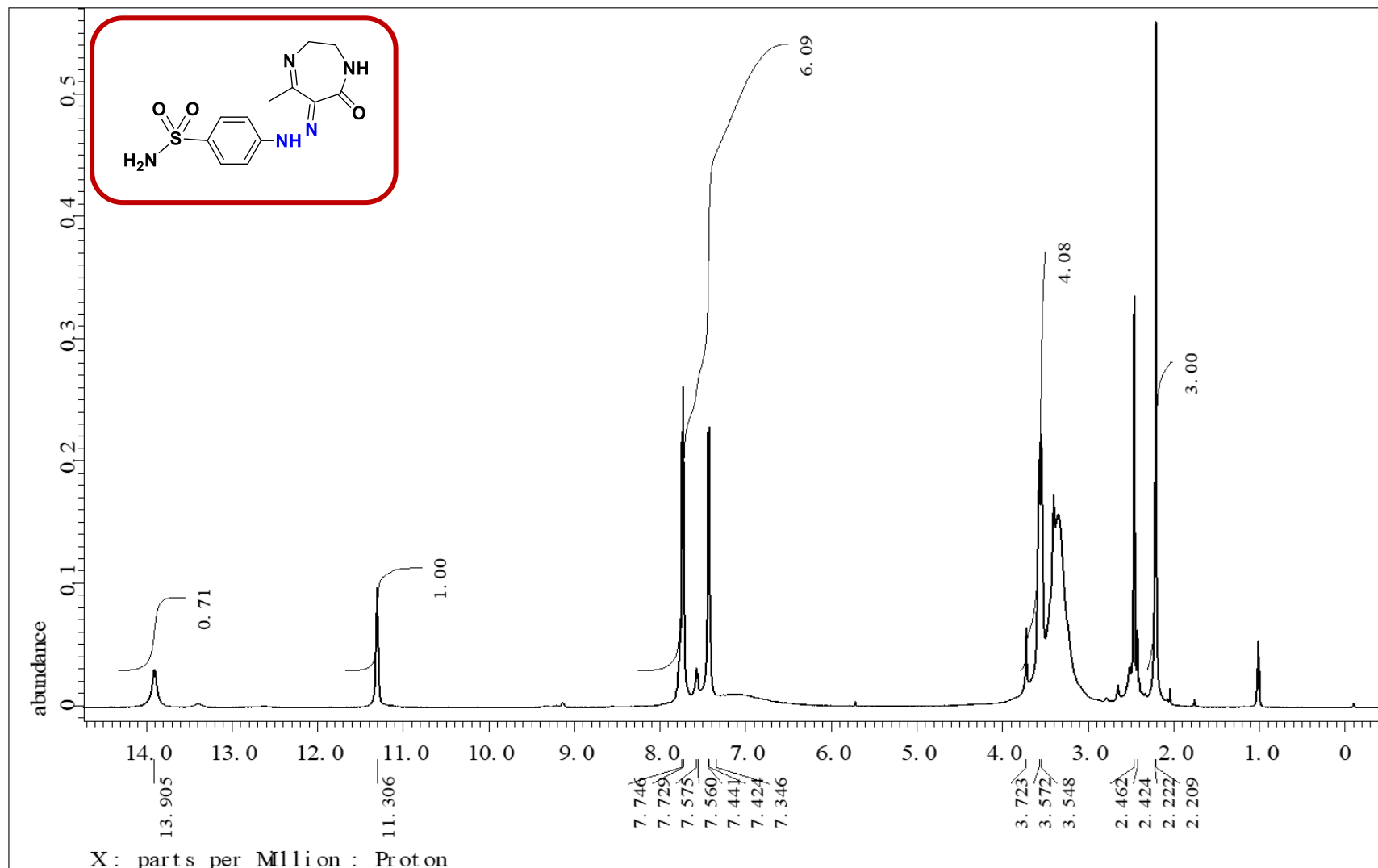


Fig. 46 ¹H-NMR spectrum (500 MHz, DMSO-d₆) of **8**.

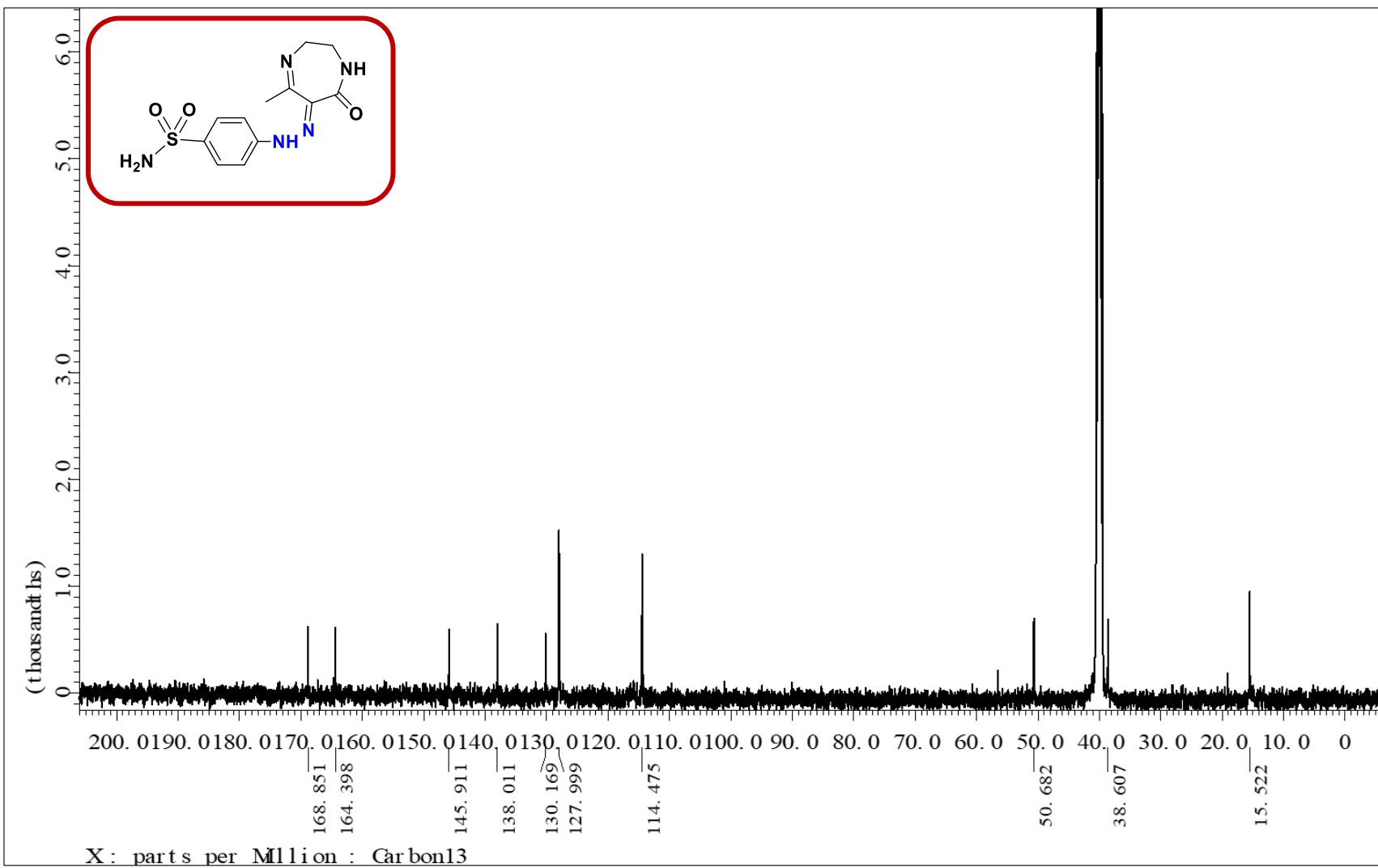


Fig. 47 $^{13}\text{C-NMR}$ spectrum (125 MHz, DMSO- d_6) of **8**.

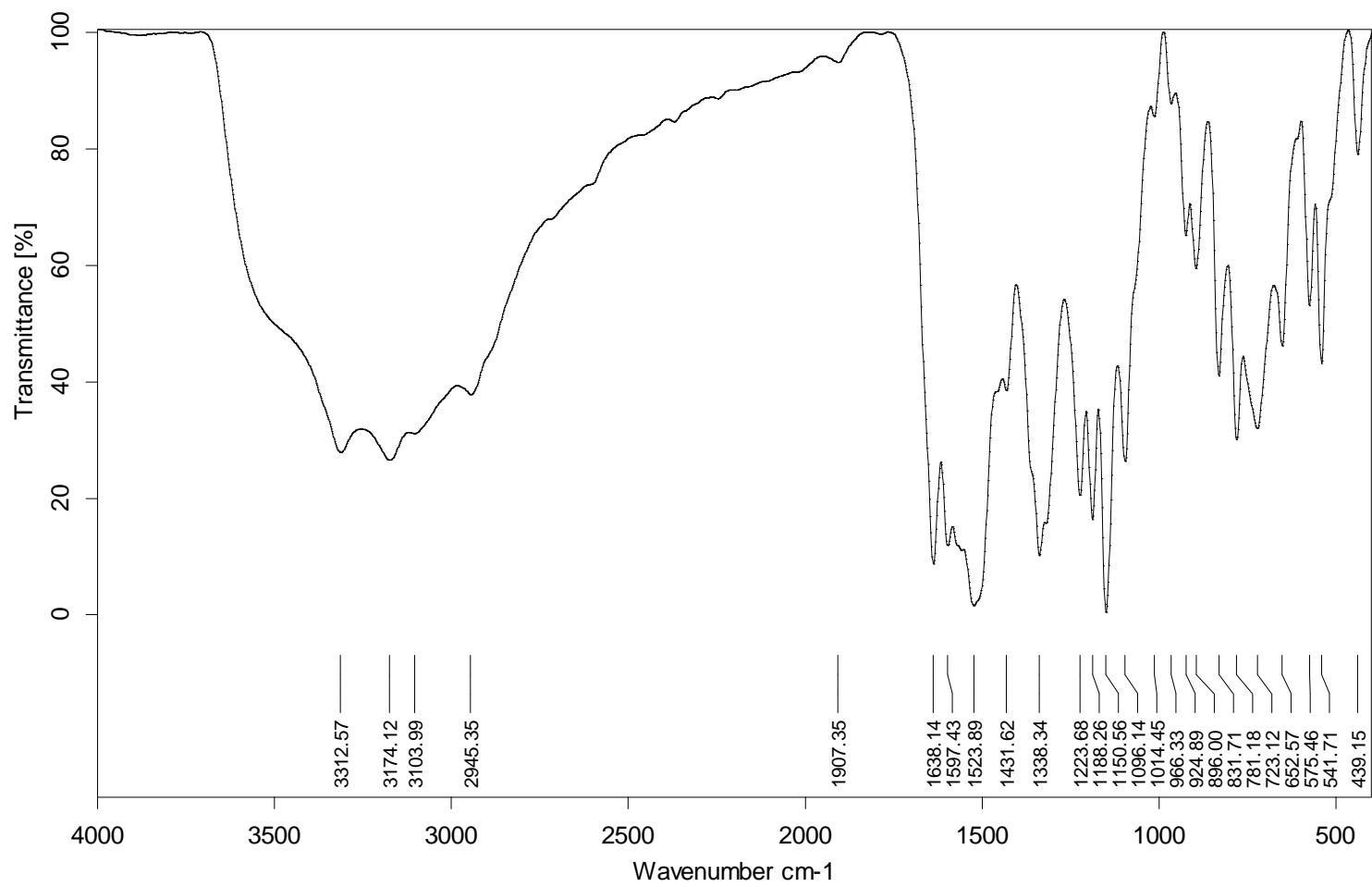


Fig. 48 IR spectrum of **8**.

2. Equipment and analytical technique

All reactions were carried out in dried glassware. NMR spectra were measured using a JEOLJNM ECA 500. The deuterated solvent was used as an internal deuterium lock. ^{13}C NMR spectra were recorded using the UDEFT pulse sequence and broad band proton decoupling at 125 MHz. All chemical shifts (δ) are stated in units of parts per million (ppm) and presented using TMS as the standard reference point. CHN analyses were performed using a Flash 2000 organic elemental analyzer. IR (KBr) ν_{max} (cm^{-1}) data were recorded using PerkinElmer; FT-IR Spectrum BX and Bruker tensor 37 FT-IR. Reaction time was Melting points were recorded using Thermo Scientific, Model NO: 1002D, 220-240v; 200 W; 50/60 Hz, and are uncorrected. Reaction time was monitored by TLC on Merck silica gel aluminum cards (0.2 mm thickness) with a fluorescent indicator at 254 nm. Visualization of the TLC during monitoring of the reaction was done by UV VILBER LOURMAT 4w-365 nm or 254 nm tube.

3. Biological procedures

Antidiabetic activity

4.3.1. Alpha-glucosidase inhibitory assay [1]

10 μL of tested compound, acarbose (positive control) or DMSO (negative control) in microtiter plate wells were mixed with 110 μL of diluted Bovine pancreatin enzyme (5 mg/0.5 mL in 0.1 M phosphate buffer at pH 7.4 then dilute 0.5 mL in 5 mL phosphate buffer). Microtiter plate wells were incubated at 37°C for 30 min. After incubation, 60 μL of maltose (1% in distilled H_2O) then incubated at 37°C for 20 min and 100 μL of glucose kit reagent (Phosphate buffer (PB, 100 mM/L); Phenol (4 mM/L); 4-aminoantipyrine (AAP, 1 mM/L); Glucose oxidase (GOD, > 20 KU/L); Peroxidase (POD, >2 KU/L) and sodium azide (NaN_3 , 8 mmol/L) were added to all wells (100 μL of phosphate buffer was added in test blank only). The absorbance was measured at 490 nm using spectrophotometer. The α -glucosidase inhibition activity of tested compound was expressed as IC_{50} . IC_{50} value (mg/mL) is the inhibitory concentration at which 50% of α -glucosidase is repressed. It was calculated by interpolation from the graph of inhibition percentage against sample concentration using linear regression equations.

4.3.2. Alpha- amylase inhibitory assay [2]

10 μL of tested compound, acarbose (positive control) or DMSO (negative control) in microtiter plate wells were mixed with 110 μL of diluted Bovine pancreatin enzyme. Microtiter plate wells were incubated at 37°C for 30 min. After incubation, 60 μL of Dextrin (1% in distilled H_2O) then incubated at 37°C for 20 min and 100 μL of glucose kit reagent (Phosphate buffer (PB, 100 mM/L); Phenol (4 mM/L); 4-amino-antipyrine (AAP, 1 mM/L); Glucose oxidase (GOD, > 20 KU/L); Peroxidase (POD, >2 KU/L) and Sodium azide (NaN_3 , 8 mmol/L) were added to all wells (100 μL of phosphate buffer was added in test blank only). The absorbance was measured at 490 nm using spectrophotometer. The α -amylase inhibition activity of tested compound was expressed as IC_{50} . IC_{50} value (mg/mL) is the inhibitory concentration at which 50% of α -amylase is repressed. It was calculated by interpolation from the graph of inhibition percentage against sample concentration using linear regression equations.

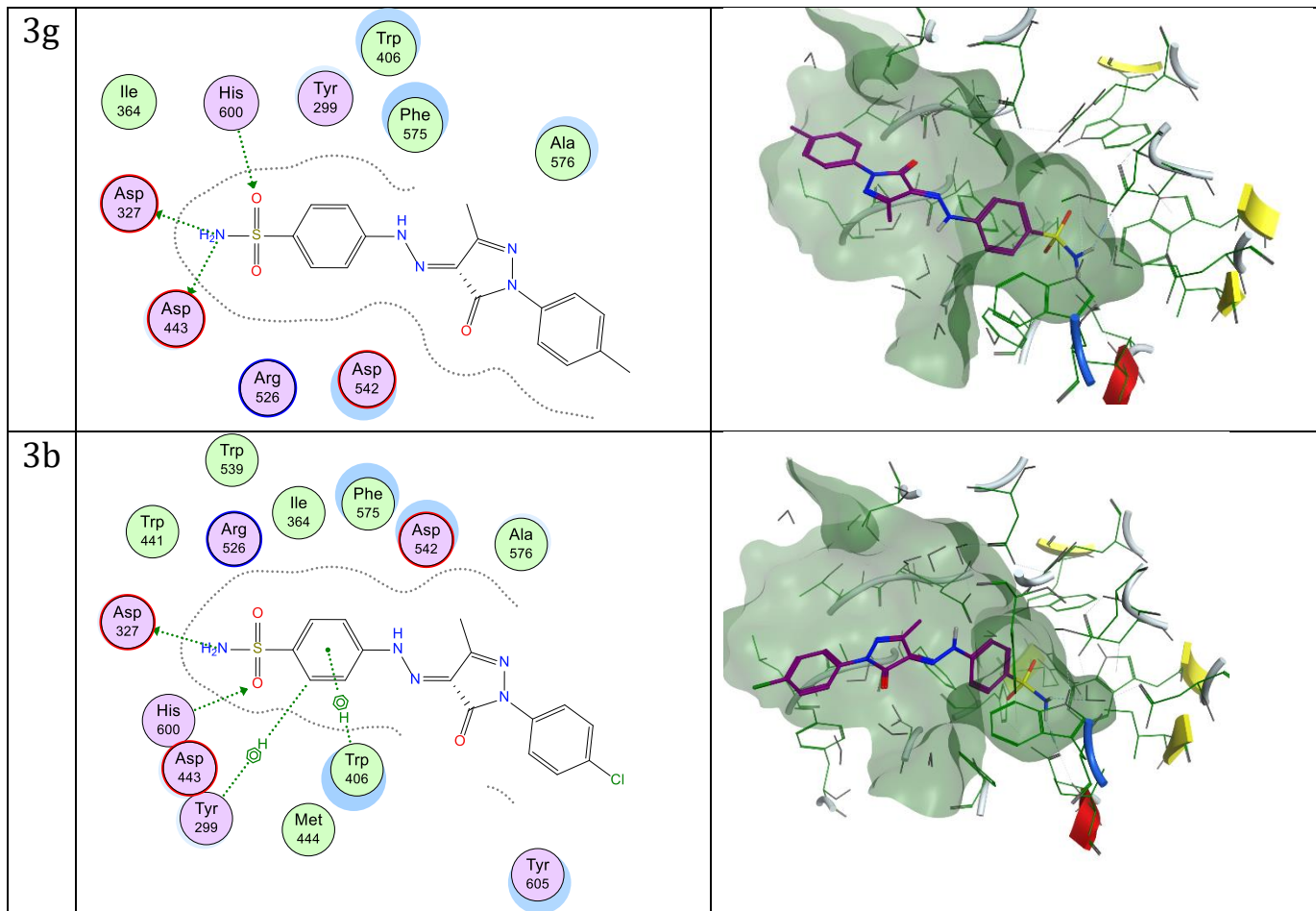
4.3.3. Glucose uptake assay [3]

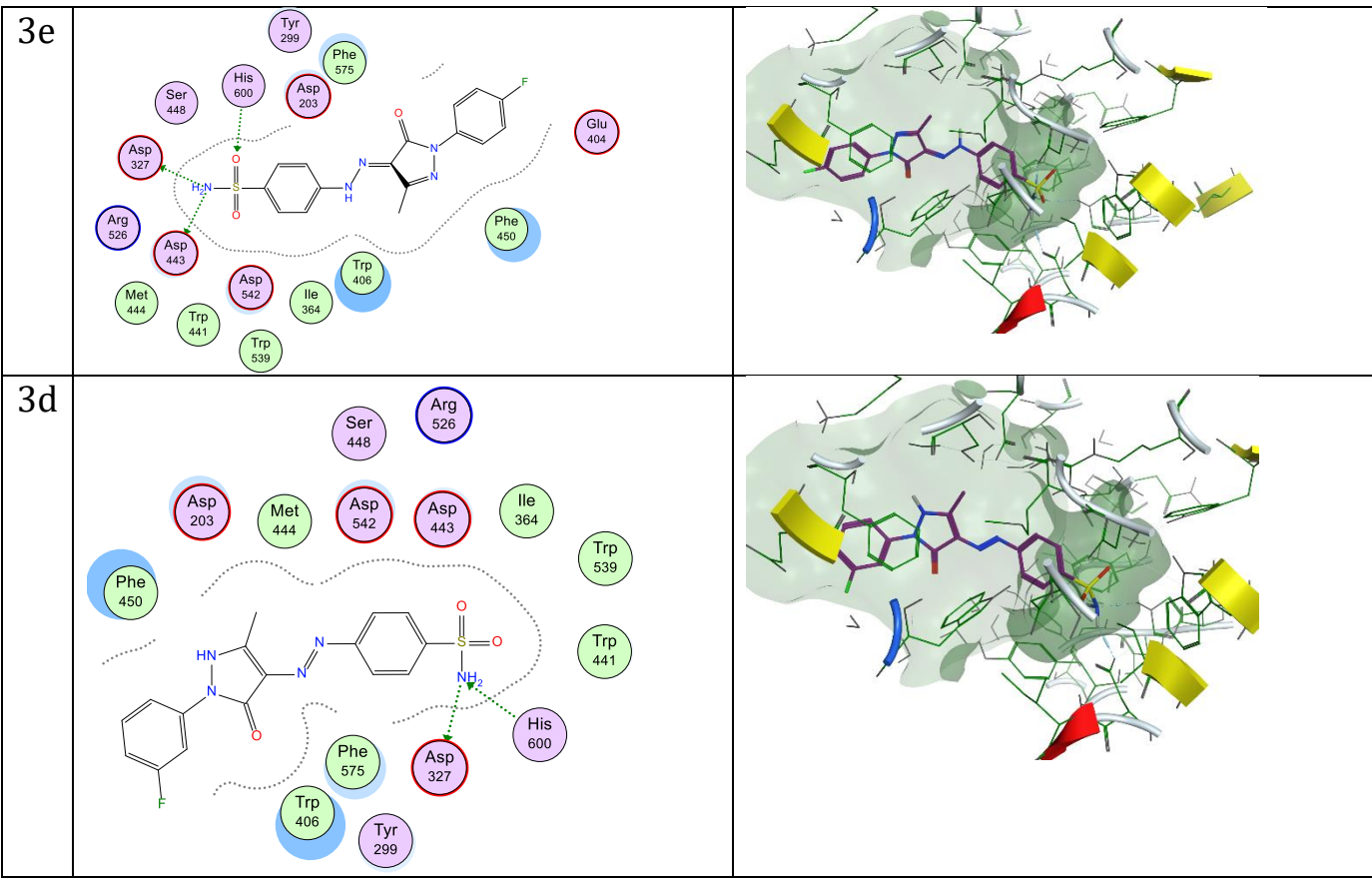
Baker yeast was washed by centrifugation ($3000 \times g$, 5min) using distilled water until the supernatant was clear and 10 % (v/v) suspension was prepared in distilled water. 1mL of tested compound, berberine (positive control) or DMSO (negative control) added to 1 mL of glucose solution (25 mM in distilled water) and incubated for 10 min at 37°C . 100 μL of yeast suspension was added and further incubated at 37°C for 60 min. All tubes were centrifuged ($2500 \times g$, 5min). The remaining glucose was estimated by glucose oxidase Peroxidase kit reagent in sample/ control tubes (phosphate buffer was added in sample blank tube) as described before. The glucose uptake of tested compound was expressed as EC_{50} . EC_{50} value (mg/mL) is the concentration at which the glucose uptake is increased by 50%. It was calculated by interpolation from the graph of glucose uptake percentage against sample concentration using linear regression equations.

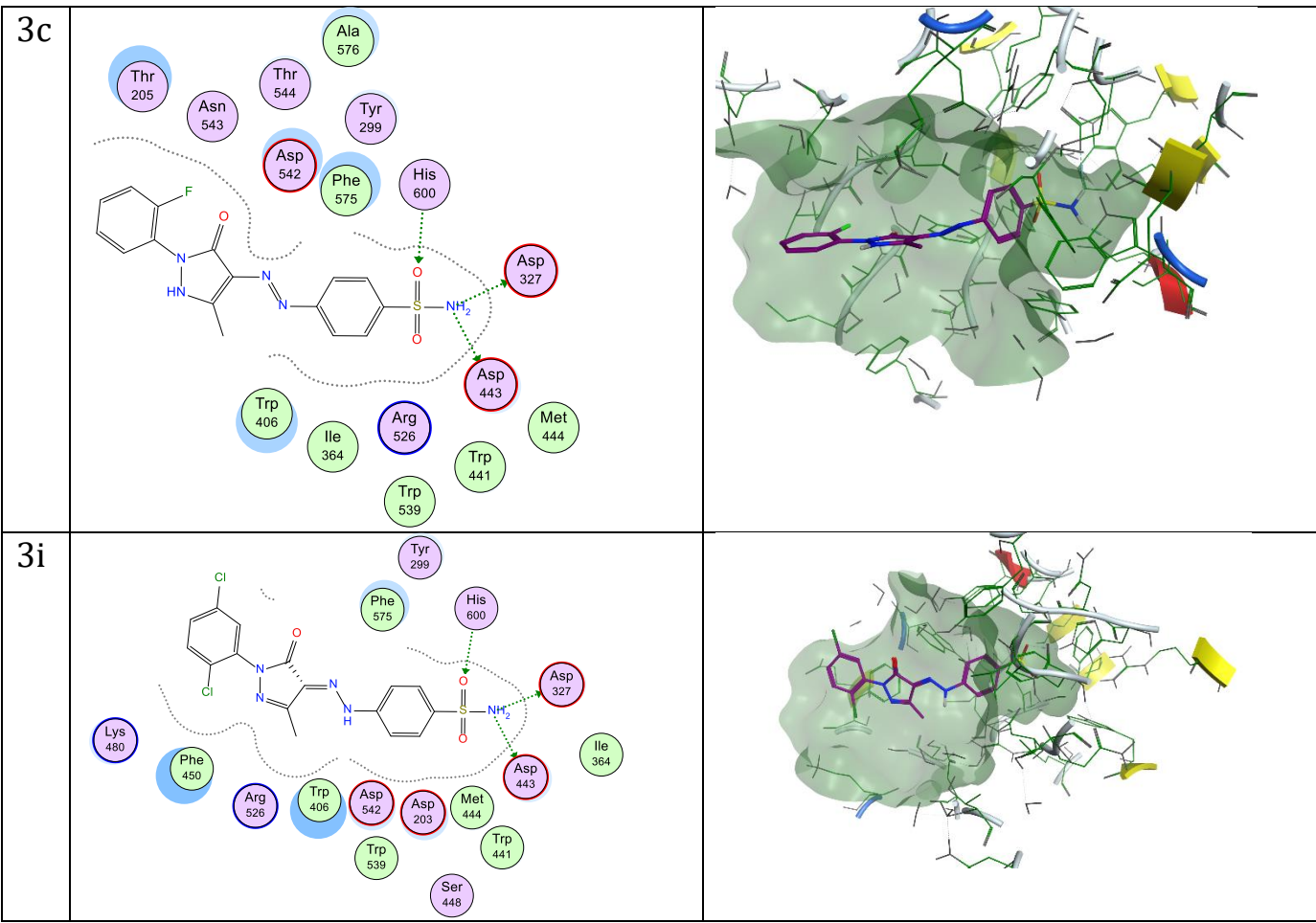
4. 2D diagram and 3D representation of molecular docking of all compounds in the binding pocket (PDB: 2QMJ)

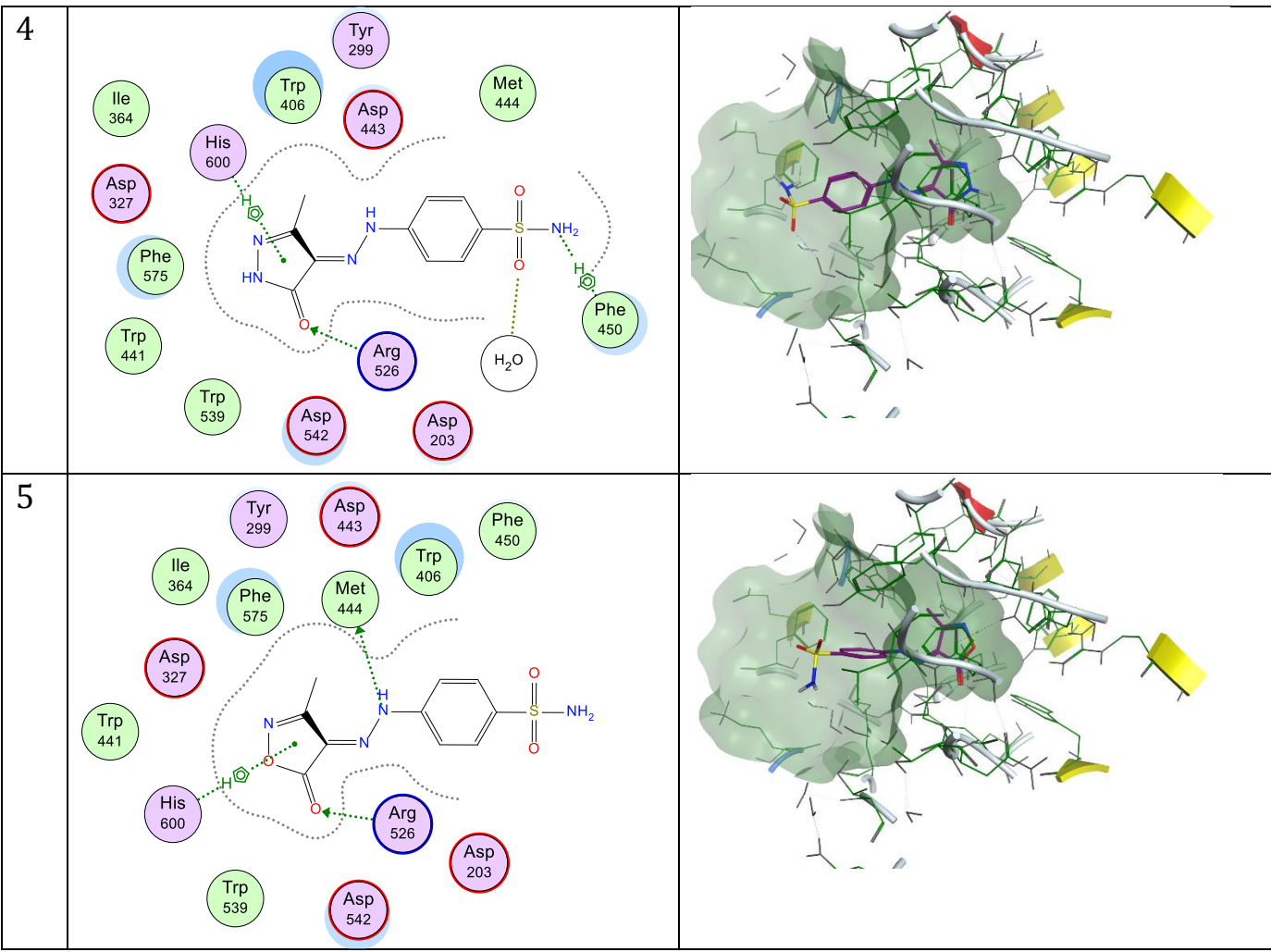
Table 1: 2D diagram and 3D representation of molecular docking of all compounds in the binding pocket (PDB: 2QMJ).

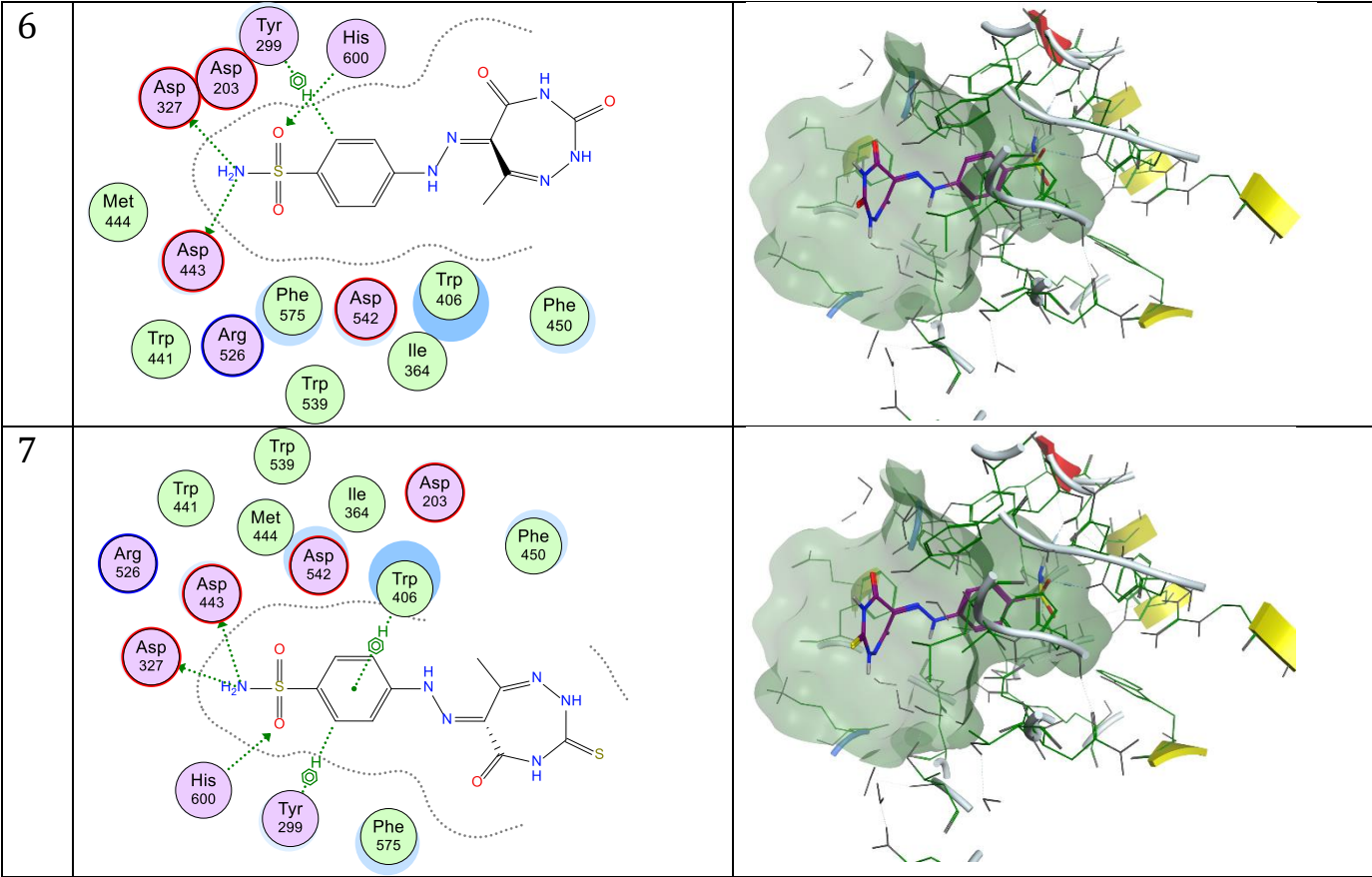
	2D interactions	3D interactions
3j		
3f		



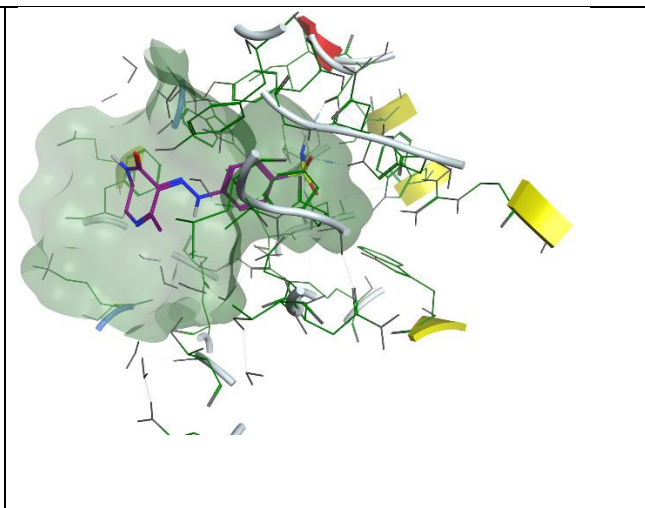
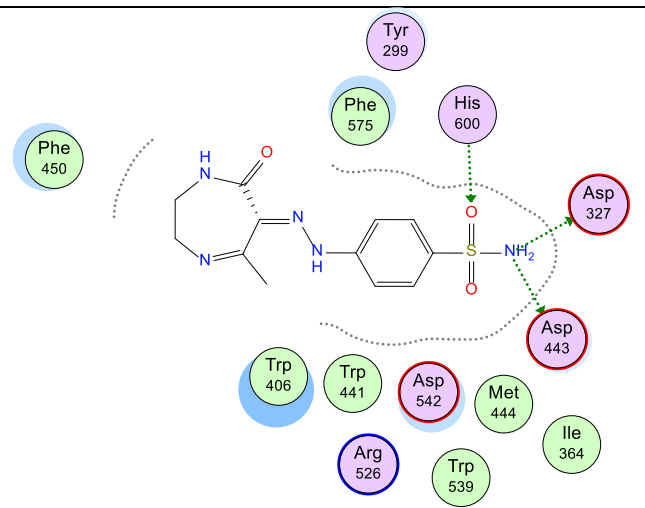








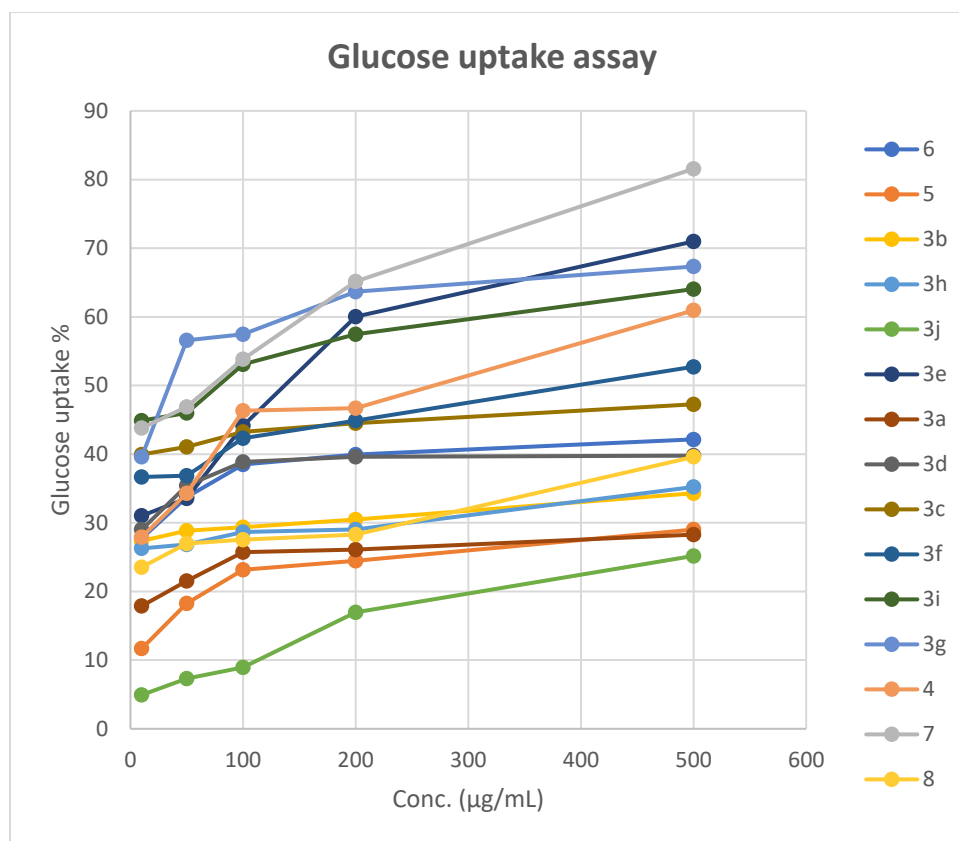
8



5. Biological activities detailed results				
Sample Code	Samples (µg/mL)	Glucose uptake	% Amylase inhibition	% Glucosidase inhibition
6	10	27.73723±0.000935414	10.17274472±0.000359139	41.86046512±0.001238144
	50	33.75912	11.13243762	46.25322997
	100	38.50365	13.243762	47.28682171
	200	39.9635	15.16314779	52.97157623
	500	42.15328	19.96161228	56.07235142
	5	10	11.67883±0.000649615	5.75815739±0.001067303
50		18.24818	9.404990403	35.4005168
100		23.17518	14.77927063	37.46770026
200		24.45255	35.8925144	40.05167959
500		29.0146	36.27639155	45.47803618
3b		10	27.37226±0.000912688	3.838771593±0.000262605
	50	28.83212	7.293666027	35.91731266
	100	29.37956	9.021113244	39.27648579
	200	30.47445	10.3646833	42.11886305
	500	34.30657	14.39539347	52.19638243
	3h	10	26.27737±0.000605805	5.75815739±0.000476546
50		26.82482	6.525911708	45.21963824
100		28.64964	8.637236084	47.54521964
200		29.0146	10.3646833	50.3875969
500		35.21898	12.85988484	54.00516796
3j		10	4.927007±0.000416569	5.37428023±0.000286556
	50	7.29927	11.13243762	36.17571059
	100	8.941606	11.70825336	41.60206718
	200	16.9708	13.05182342	43.15245478
	500	25.18248	19.00191939	60.98191214
	3e	10	31.0219±0.00070214	6.525911708±0.000189785
50		33.57664	8.253358925	37.46770026
100		44.16058	11.13243762	39.01808786
200		60.0365	13.243762	41.86046512
500		70.9854	13.81957774	42.37726098
3a		10	17.88321±0.000684376	22.6487524±0.000136057
	50	21.53285	22.84069098	36.69250646
	100	25.72993	23.03262956	37.98449612

	200	26.09489	25.33589251	40.05167959
	500	28.28467	27.44721689	50.12919897
3d	10	29.0146±0.001213211	16.89059501±0.000382964	25.06459948±0.000863134
	50	35.40146	18.04222649	27.64857881
	100	38.86861	18.42610365	30.49095607
	200	39.59854	19.19385797	37.72609819
	500	39.78102	20.92130518	40.31007752
3c	10	39.9635±0.000790569	6.333973129±0.000334183	32.81653747±0.000577062
	50	41.05839	11.90019194	34.88372093
	100	43.24818	14.39539347	38.50129199
	200	44.52555	16.12284069	42.63565891
	500	47.26277	16.69865643	45.73643411
3f	10	36.67883±0.001104482	14.39539347±0.000238419	28.68217054±0.000696419
	50	36.86131	17.27447217	31.00775194
	100	42.33577	21.88099808	33.33333333
	200	44.89051	22.26487524	40.31007752
	500	52.73723	22.6487524	44.18604651
3i	10	44.89051±0.000998499	14.39539347±0.000264627	28.94056848±0.001095445
	50	45.9854	17.27447217	30.74935401
	100	53.10219	18.04222649	33.33333333
	200	57.48175	18.61804223	35.14211886
	500	64.05109	21.6890595	38.50129199
3g	10	39.59854±0.000981326	24.37619962±0.000929425	27.39018088±0.000878635
	50	56.56934	25.14395393	32.04134367
	100	57.48175	25.52783109	35.14211886
	200	63.68613	26.67946257	38.50129199
	500	67.33577	31.66986564	44.44444444
4	10	27.91971±0.001379493	8.637236084±0.000273287	24.54780362±0.001167048
	50	34.30657	12.85988484	29.71576227
	100	46.35036	13.62763916	37.98449612
	200	46.71533	14.77927063	38.75968992
	500	60.94891	34.74088292	39.01808786

7	10	43.79562± 0.000875785	11.90019194± 0.000742389	22.73901809± 0.000673053
	50	46.89781	13.81957774	29.97416021
	100	53.83212	15.54702495	31.26614987
	200	65.14599	17.46641075	35.4005168
	500	81.56934	19.57773512	36.69250646
8	10	23.54015± 0.001837662	9.596928983± 0.000227306	40.05167959± 0.00069857
	50	27.0073	10.94049904	40.82687339
	100	27.55474	13.05182342	45.99483204
	200	28.28467	14.01151631	47.80361757
	500	39.59854	15.93090211	65.89147287



6. References

- [1] T. Matsui, C. Yoshimoto, K. Osajima, T. Oki, Y. Osajima, In Vitro Survey of α -Glucosidase Inhibitory Food Components, *Biosci. Biotechnol. Biochem.* 60 (1996) 2019–2022. doi:10.1271/bbb.60.2019.
- [2] K. Lalitha, V.K. Kumar, In vitro study on α -amylase inhibitory activity of an Ayurvedic medicinal plant, *Anacyclus pyrethrum* DC root, *Indian J. Pharmacol.* 46 (2014) 350. doi:10.4103/0253-7613.132204
- [3] V.P. Cirillo, MECHANISM OF GLUCOSE TRANSPORT ACROSS THE YEAST CELL MEMBRANE, *J. Bacteriol.* 84 (1962) 485–491. doi:10.1128/jb.84.3.485-491.1962.